Design of an Expandable In-Pedicle Anchor for Spinal Fusion Surgery

The design, manufacturing, and validation of a proof-of-principle prototype

Master Thesis

Cornel Weststeijn

Delft University of Technology

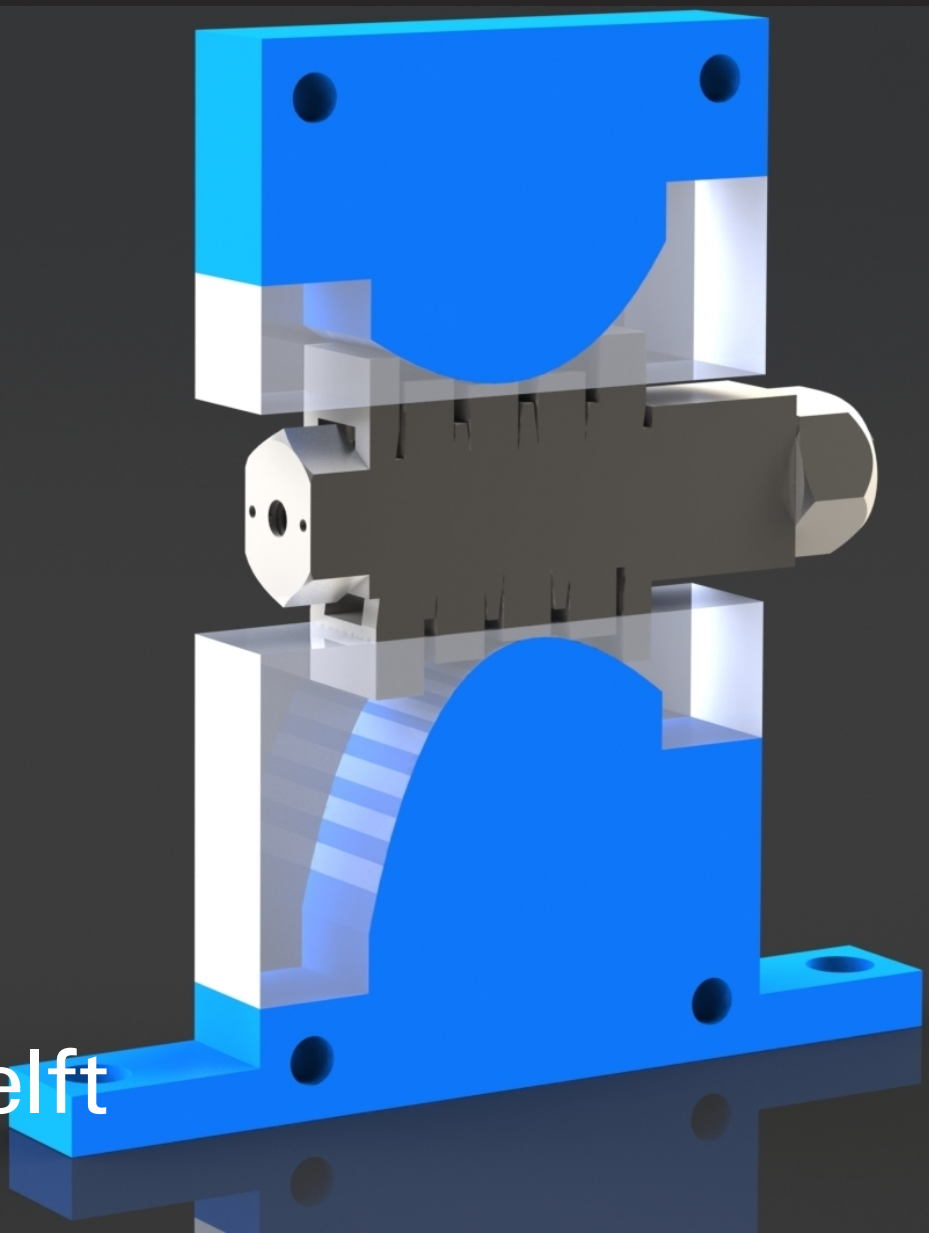

TU Delft

Design of an Expandable In-Pedicle Anchor for Spinal Fusion Surgery

The design, manufacturing, and validation of a proof-of-principle prototype

by

Cornel Weststeijn

to obtain the degree of Master of Science
at the Delft University of Technology
to be defended on 24-05-2022.

Student Number:	4462580	
Master:	Mechanical Engineering	
Track:	BioMechanical Design	
Course Code:	ME51032	
Thesis Committee:	de Kater, E.P.	Daily Supervisor
	Breedveld, P.	Chair
	Horeman, T.	Graduation Committee

TU Delft

Abstract

Loosening of pedicle screws after spinal fusion surgery can lead to serious complications and may prevent fusion between vertebrae. This problem, which has increased in recent years, is a more frequent problem in patients with osteoporosis. In this study, we explore the possibility to use an expanding in-pedicle anchor with the goal of increasing the contact area of the in-pedicle anchor with the pedicle cortex to reduce toggling. Toggling is the rocking motion that can occur when an in-pedicle anchor is subjected to lateral forces that can occur during the patient's daily activities. A stainless steel scaled-up 2D proof-of-principe prototype was developed and manufactured consisting of a central bolt with flattened sides, a nut, and ten sliding wedges. The wedges expand by applying a compression force by tightening the nut. In order for the prototype to reach the pedicle cortex, it needs to compress the surrounding cancellous bone first. It was shown in experiments that the proof-of-principle prototype was able to compress 5 and 10 PCF Sawbones solid foam, which corresponds to osteoporotic human cancellous bone. The proof-of-principle prototype was able to make contact with the top and bottom of a custom-made 2D pedicle model where a conventional screw would have been limited to contact on the two flanks. The proof-op-principle prototype showed a better resistance to lateral loads than an unexpanded model with the same dimensions. The proposed in-pedicle anchor shows potential for improved resistance to caudocranial toggling by increasing the number of contact points with the pedicle cortex. The use of an in-pedicle expansion to prevent toggling holds a promising future for possible clinical applications.

Acknowledgements

It is a strange feeling to realize that this thesis concludes my education at TU Delft and that it is time for the next step. A project of this length, which I really enjoyed, is both a shame and a blessing to end. As a starting bachelor's student, I looked up to people that graduated and obtained their master's degree, but now I am one of them. Luckily, new challenges lie in front of me that I can tackle with the knowledge gained at TU Delft.

Firstly, I want to thank my daily supervisor, Esther. By talking to other students, I realized that it is not self-evident to have a thesis supervisor who is always there for discussions when you need it. Thank you for the weekly meetings, guidance, and small pep talks when I needed them. I am also grateful for Paul's creative input during the brainstorming sessions and the rich knowledge of wonderful mechanisms that he displayed at every meeting.

I want to thank my roommates, friends, family, and girlfriend for sparring about my thesis, proofreading the text, just listening to my frustrations in the last months, or studying together at the BK faculty together. Especially in corona times, it was nice to have such a great group of friends around me to stay motivated by studying together.

Lastly, I want to thank David from DEMO for manufacturing an excellent prototype of my design. The collaboration was very pleasant and it is wonderful to see his craftsmanship reflected in the prototype.

C.F. Weststeijn
Delft, May 2022

Contents

1 Introduction **1**
- 1.1 Background . . . 1
  - 1.1.1 Spinal Fusion Surgery . . . 1
  - 1.1.2 Spinal Fusion Procedure and Instrumentation . . . 1
  - 1.1.3 Spinal Anatomy . . . 2
- 1.2 Problem Definition . . . 4
  - 1.2.1 Failing Mechanism . . . 4
  - 1.2.2 Current Solutions . . . 4
- 1.3 Functions of an in-pedicle anchor . . . 4
  - 1.3.1 Fixation . . . 4
  - 1.3.2 Perforation . . . 5
  - 1.3.3 Insertion: Supportive function . . . 5
  - 1.3.4 Rigid connection and force transfer: Supportive function . . . 5
  - 1.3.5 Connection point for correction rods or plates: Supportive function . . . 5
- 1.4 Target pedicle model . . . 5
  - 1.4.1 Choice for L1 vertebra . . . 5
  - 1.4.2 Simplified pedicle model . . . 6
- 1.5 Project Goal . . . 6
- 1.6 Structure of the Report . . . 6

2 Requirements **7**
- 2.1 Functional requirements . . . 7
- 2.2 Geometric requirements . . . 7
- 2.3 Wishes . . . 7

3 Conceptual Design of the In-Pedicle Anchor **8**
- 3.1 Categorization of Expansion Working Principles . . . 8
- 3.2 Selection of Expansion Working Principles . . . 8
  - 3.2.1 Assessment requirements . . . 8
  - 3.2.2 Rating of Categories . . . 9
  - 3.2.3 Final verdict . . . 10
- 3.3 In-Pedicle Anchor Concept Generation . . . 10
  - 3.3.1 Concept 1: Stars . . . 10
  - 3.3.2 Concept 2: Wedges . . . 10
  - 3.3.3 Concept 3: Plug . . . 11
- 3.4 Selection of In-Pedicle Anchor Concepts . . . 11
  - 3.4.1 Toggling Experiment . . . 11
  - 3.4.2 Concept Selection . . . 12

4 Detailed Design of the Final In-Pedicle Anchor Prototype **13**
- 4.1 Working Principle of the In-Pedicle Anchor Prototype . . . 13
- 4.2 Theoretical Friction Analysis . . . 13
- 4.3 Final Prototype Design . . . 14
  - 4.3.1 2D Simplification of Prototype . . . 14
  - 4.3.2 Manufacturing of Prototype . . . 15

5 Experimental Validation of the In-Pedicle Anchor Prototype 16
5.1 Experiment 1: Cancellous Bone Compression . . . 16
5.1.1 Experiment Goal . . . 16
5.1.2 Experiment Variables . . . 16
5.1.3 Experimental Facility . . . 17
5.1.4 Experiment Protocol . . . 17
5.1.5 Data Analysis . . . 17
5.2 Experiment 2: In-pedicle expansion and lateral loading . . . 17
5.2.1 Experiment Goal . . . 17
5.2.2 Experimental Variables . . . 18
5.2.3 Experimental Facility . . . 18
5.2.4 Experimental Protocol . . . 19
5.2.5 Data Analysis . . . 19

6 Results 19
6.1 Experiment 1: Cancellous Bone Compression . . . 19
6.2 Experiment 2: In-pedicle expansion and lateral loading . . . 21

7 Discussion 21
7.1 Main findings . . . 21
7.2 Limitations and Future Research . . . 21
7.2.1 Design . . . 21
7.2.2 Validation Experiments . . . 26

8 Conclusion 27

References 29

Appendix A: Design of Simplified Pedicle Model 30

Appendix B: Concept Prototype Experiments 32

Appendix C: Friction Calculations 36

Appendix D: Raw Data Validation Experiments 38

Appendix E: Technical Drawings Final Prototype 40

1. Introduction

1.1. Background

1.1.1. Spinal Fusion Surgery

Spinal Fusion Surgery is a procedure used to improve stability, correct deformities, or reduce pain in the spine. The number of spinal fusion surgeries doubled between 2010 and 2018, making it the sixth most common inpatient surgery in the US [1]. Spinal Fusion Surgery is also the most expensive surgical procedure in the US in terms of aggregate hospital costs, with a total yearly cost of around $14.1 billion [2]. In the past years, the number of spinal fusions has steadily increased from an estimated 203.053 in 2008 to 442.776 in 2014 in the US alone [3]. This surgery is mostly performed in cases of spinal or disk degeneration and spinal stenosis, which is the narrowing of the intervertebral spaces in the spine. This can lead to compression or irritation of the spinal cord. Other uses can be a spinal correction in patients with spinal instability, such as scoliosis. Scoliosis is a condition that manifests itself as a lateral c- or s-shaped bend in the spine. Spinal instabilities such as scoliosis not only harm the posture and mobility of the patient but can also lead to more severe neurological symptoms when the spinal cord is compromised [4]. Spinal fusion is used to permanently connect two or more adjacent vertebrae in the spine, eliminating motion between them. This is done by using bone graft material to bridge the gap between the two adjacent bone joint surfaces and stimulate bone growth to permanently fixate the painful or deformed joint.

1.1.2. Spinal Fusion Procedure and Instrumentation

To keep the joint from moving and give the bone graft time to heal, metal screws and plates or rods are used to fixate two or more vertebrae to each other. The metal screws are screwed into the vertebra to provide an attachment point for the plates or rods. These rods or plates connect the unstable vertebral elements to a stable element of the spine. Figure 1.1 shows a spinal fusion construct outside of the body, and both a schematic drawing and a CT scan of it inside the body. Older methods of Spinal Fusion Surgery used hooks and wires to fixate the unstable spinal elements. Nowadays mostly screws are used due to their superior load-bearing capacity in all directions, but in certain cases, hooks and wires can be used for fixation.

During the surgery, the insertion point for the screw is determined based on anatomical landmarks. These anatomical landmarks can differ per vertebra along the spine. Then the bone cortex at the entry point is opened with a surgical burr. Using a pedicle probe a track is made following the central axis of the pedicle through the isthmus into the vertebral body. Ideally, the tracks should be fully horizontal in the transverse plane and converge towards each other. The track is then checked using a pedicle sound that uses electrical conductivity to check whether the cortex is pierced [5]. Lastly, a screw with the right diameter and length is inserted following the created trajectory.

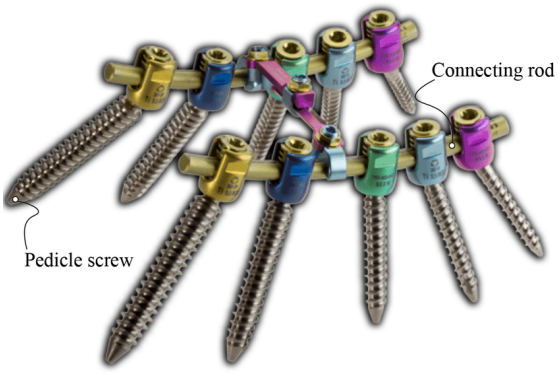

(a) *Pedicle screws and connecting rods used in Spinal Fusion Surgery.*

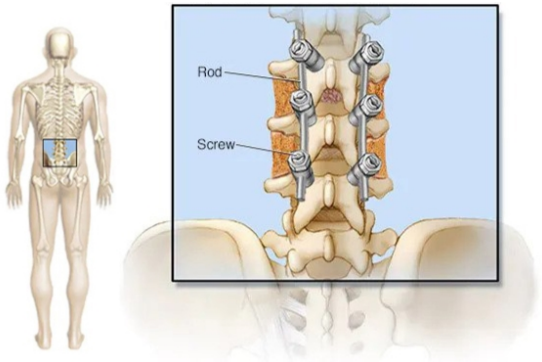

(b) *Schematic drawing including the anatomical location on the left [6].*

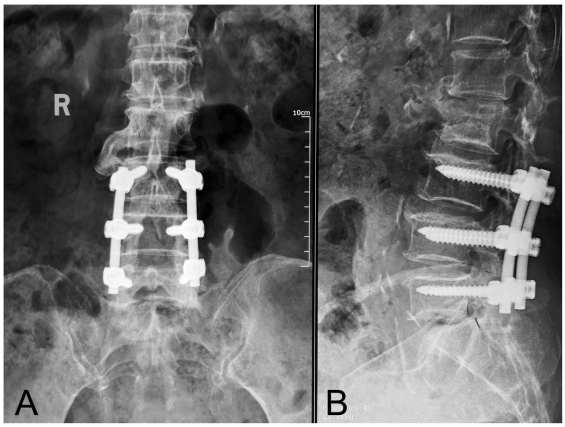

(c) *Anterior-posterior (A) and lateral (B) x-rays of the spinal construct [7].*

Figure 1.1: *Depictions of instrumentation and placement of a posterior lumbar spinal fusion.*

A longer screw provides more stability, but the screw should not perforate the anterior cortex of the vertebral body to prevent serious complications such as aortic injury. The pedicle screw diameter (SD) should provide enough contact with the pedicle cortex, without breaking it. Pedicle screws are, therefore, available in different lengths and diameters, so both dimensions of the screw can be chosen from the available sizing system. The choice of the screw size is based on the dimensions and specific anatomy of the pedicle which can be seen and measured on the CT scan. There is not one specific criterium for pedicle SD selection, but one rule of thumb that is named in some literature is that the screw diameter should be 80% of the pedicle width [8, 9]. Often surgeons also pre-tap the hole with a tap that has a diameter that is 0.5 or 1 mm smaller than the screw that is going to be placed [10]. These pedicle screws get 60-80% of their stability from the hard cortical outer bone layer called the pedicle cortex. The rest is supported by the soft inner cancellous bone of the vertebral body [11]. A proper fixation in cortical bone is even more important for patients with osteoporosis. Osteoporosis is a disorder that deteriorates bone and especially compromises cancellous bone. Some studies claim loosening rates in osteoporotic patients of 12.9% [12]. Because of this, research is also being conducted into other insertion trajectories that could have more contact with cortical bone [13].

1.1.3. Spinal Anatomy

The spine or vertebral column is the supportive core where all other parts of the musculoskeletal system are connected to and ensures that humans can stand erect and move. It also houses and protects the spinal cord, which carries nerve signals throughout the body to allow sensing and movement. The spine is schematically depicted in Figure 1.2. The spine consists of 33 vertebrae, of which the 24 upper vertebrae are flexibly connected and separated by a disc, and the lower 9 vertebrae are fused in the sacrum (5) and the coccyx (4). The 24 upper vertebrae are divided into cervical (7), thoracic (12), and lumbar vertebrae (5). The different vertebrae roughly have the same anatomy, but all have irregular complex structures. The general anatomy of a thoracic vertebra is depicted in the illustrations in Figure 1.3. Vertebrae consist of two main parts: the anterior vertebral body and the posterior part called the vertebral arch. The hole in the middle of the vertebra is called the vertebral foramen and houses the spinal cord [14].

The biggest part of the vertebra is the vertebral body which is a thin-walled structure of cortical bone filled with softer, cancellous bone. The other major part, the vertebral arch, consists of multiple bone structures: one spinous process, two transverse processes, four articular processes, and two pedicles. The spinous and transverse processes act as attachment points for muscles and ligaments. The articular processes fit on the adjacent vertebrae to provide stability and mobility in the desired directions. The two pedicles have a complex shape that is hard to capture quantitively. This is why Panjabi *et al.* [15] decided to create a computer-generated surface model of a thoracic pedicle using an optoelectronic digitizer. Figure 1.4 shows the model of the outer surface of the pedicle, which shows the true complexity of the shape. Many other studies simplify the pedicle into an oval cylindrical model. However, this does not do justice to the complex shape and the practical problems in the use of pedicle screws that can arise as a result.

The diameter of an L1 lumbar pedicle consists of around 30 % cortical bone [16]. This means that the cortical thickness is much larger in the pedicle than in the vertebral body. Cortical bone is more resistant to local stresses and therefore more suitable for fixation of, for example, a pedicle screw. Due to this high proportion of cortical bone, most screws are inserted in the pedicle. The most used insertion trajectory follows the central axis of the pedicle into the vertebral body.

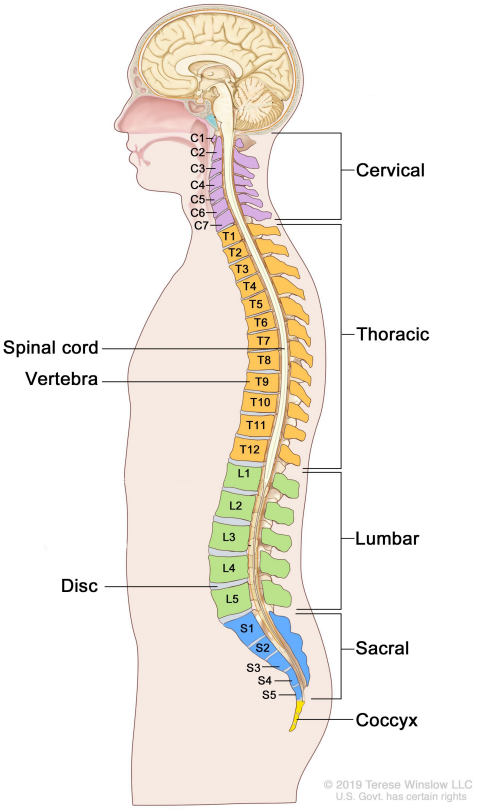

Figure 1.2: *Depiction of the human spine including the anatomical terminology [17].*

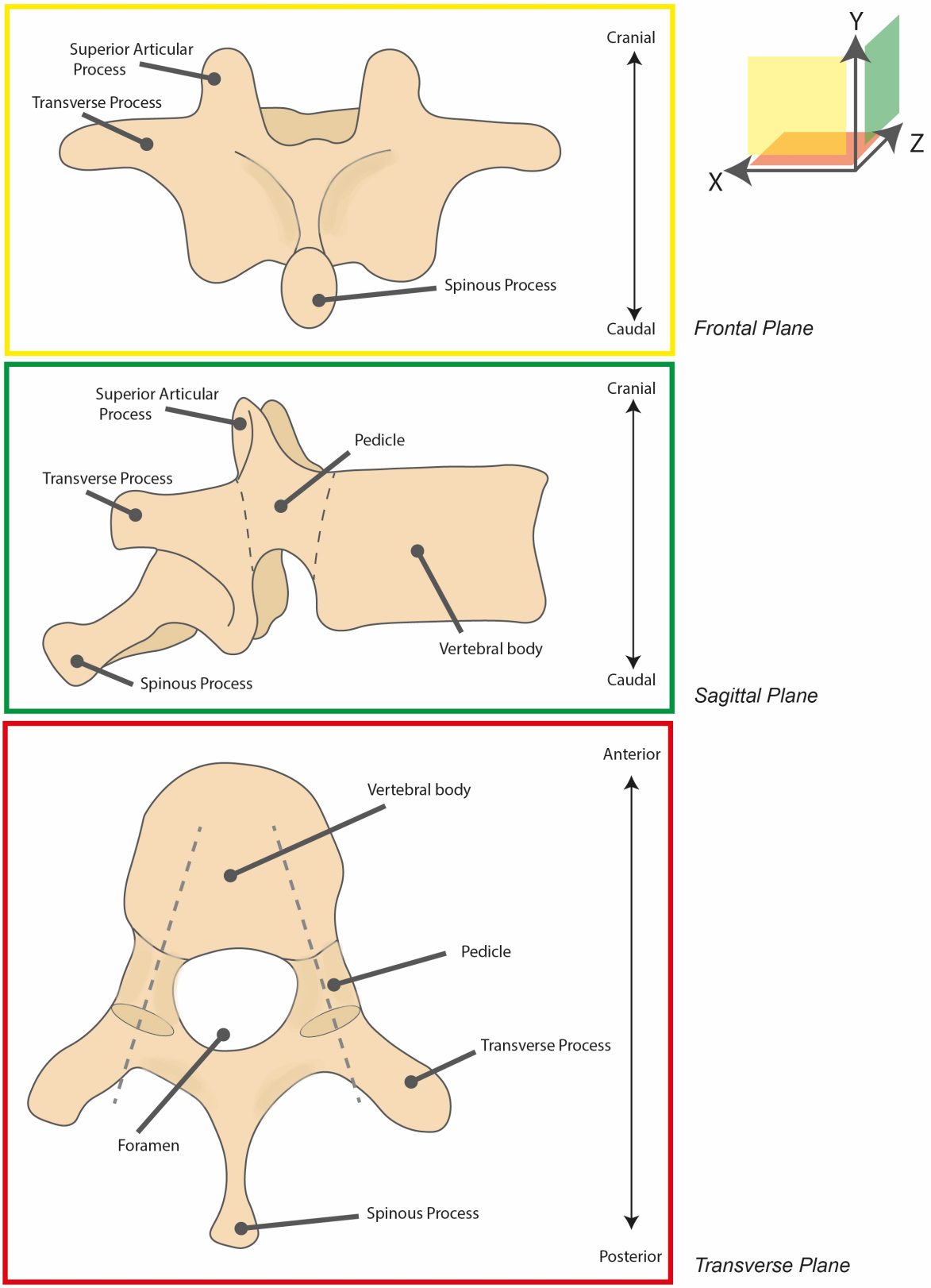

Figure 1.3: *Vertebral Anatomy.*

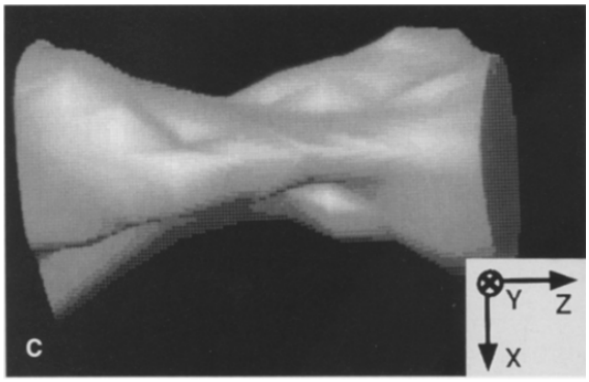

Figure 1.4: *Surface model of the Pedicle [15].*

1.2. Problem Definition

1.2.1. Failing Mechanism

Screw loosening is a major failure mechanism and the number of cases has been increasing in recent years [18, 19, 20]. Studies have looked at the average time for these implants to loosen, which is an average of three to six months [21]. Together with information about the wear pattern and observed fail patterns, this has led to the conclusion that loosening mainly occurs due to cyclic loads. This is also the reason that cyclic loading is nowadays assumed to be a more clinically relevant testing method than pull-out tests which just measure the required force to pull the screw out of the vertebrae axially [22].

Although the exact working of this failure mechanism under cyclic loading at the micro-level is not completely clear, the failure mechanism is hypothetically described by Choma et al. [23] as 'localized irreversible compressive yield or viscoelastic creep of the osteoporotic bone and/or shear slip between interface or fracture surfaces that progressively propagates each loading cycle that reaches or exceeds a threshold force.' Due to this cyclic caudocranial loading, a butterfly-shaped hole is created in the cancellous bone. This can happen because of the complex shape of the pedicle. The screw rocks about the smallest point of the pedicle; the isthmus. The contact area between the screw threads and the cortical pedicle wall at this isthmus is minimal. According to Verdult [16], it is limited to two flanks of the screw due to the oval shape of the pedicle. This results in a small contact area that makes the pedicle screw vulnerable to transverse forces both in the ventrodorsal and caudocranial direction. Because the attachment points in the cortical bone are on the sides, the rocking movements caused by caudocranial forces are the largest as shown in Figure 1.5.

Loosening of a screw is often demonstrated with a radiographic image. In these images a spot or 'halo' forms around the screw. This radiographic halo is connective tissue and not the desired bone. It has been shown that when screw movement occurs, the natural response is to produce connective tissue and initiate bone resorption. Especially in the first six weeks after surgery there must be as little movement as possible to allow the bone to recover and to allow bone to grow and encapsulate the in-pedicle anchor.

1.2.2. Current Solutions

Several approaches are used to prevent screw loosening. The use of a larger diameter or length screw, the use of screws with a wider neck, or the application of bone cement. The use of bone cement to improve the pullout strength and the toggling resistance of the screw has an effect. The use of cemented screws can lead to 63% less caudocranial motion [24]. Unfortunately, the use of bone cement has several drawbacks. Removal of the pedicle screw may be necessary in case the screw causes discomfort for the patient or there are more serious complications such as infections. It is, however, very difficult to remove an implant reinforced with bone cement, because there will always be residual bone cement in the cancellous bone. In addition, the exothermic reaction that takes place during the curing of the bone cement can cause high temperatures that can lead to bone necrosis. Finally, in the event of a leak, bone cement can flow out of the bone and into the vertebral foramen, which can lead to neurological damage if nerves are affected. None of the offered solutions focuses on adapting the macro shape to the surrounding pedicle thereby trying to prevent this toggling motion, except for cement augmentation with its obvious drawbacks.

1.3. Functions of an in-pedicle anchor

1.3.1. Fixation

The main goal of the pedicle screw is to fixate itself in the surrounding bone. This fixation is provided through a shape-lock of the screw threats in the surrounding bone. This fixation can also be achieved in different ways. An overview is made of the different ways of fixation in Figure 1.6. As explained in Section 1.2 the toggling happens due to a small contact area between the screw threads and the cortical pedicle wall. Therefore, this project focuses on fixation by adapting the macro shape of the anchor to the internal shape of the pedicle, to enlarge the contact area along the length of the in-pedicle anchor. If we want to enlarge this contact area also behind the isthmus we need an anchor that can fit through the isthmus and then expands. Therefore, the focus will lay on the use of expansion to adapt the macro shape of the in-pedicle anchor to the pedicle cortex.

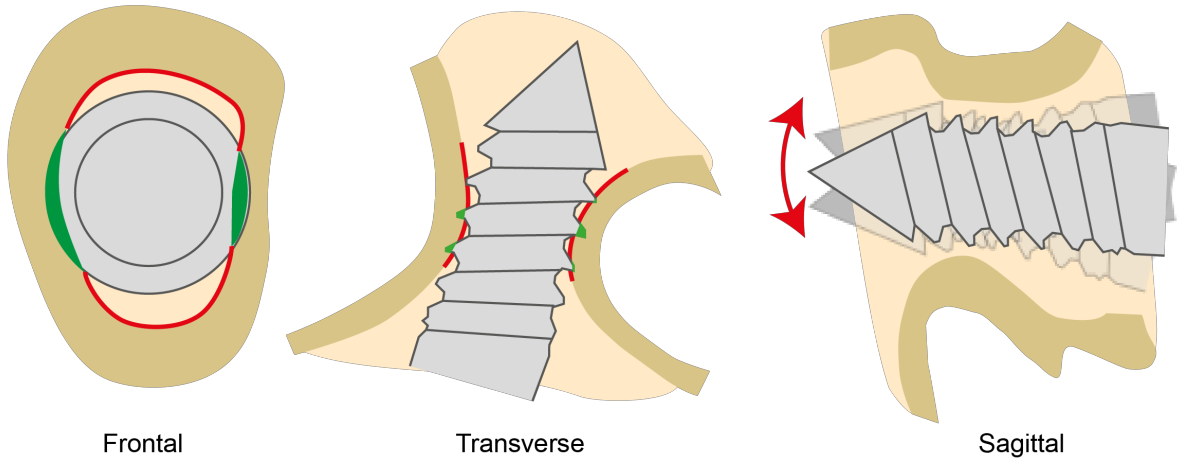

Figure 1.5: *Depiction of a pedicle screw in the pedicle and its fixation. The penetration area of the screw in the cortical bone is shown in green and the theoretical maximum contract area with the cancellous bone in red.*

1.3.2. Perforation

Perforation of cortical bone is only a required feature for micro shape-locking systems such as conventional pedicle screws. The threads of the pedicle screw perforate the surrounding cortical bone to create a cavity where the threads of the screw fit in, allowing a shape lock between the bone and the pedicle threads. In the case of a screw, an internal thread is tapped into the surrounding bone when it is screwed inside the bone, but there are other ways to create these cutouts. Other systems might use a perforation system only for penetration of cancellous bone to create space for expansion, but not for cortical bone.

1.3.3. Insertion: Supportive function

The in-pedicle anchor has to be inserted into the bone to the right depth to allow it to lock in the shape-locking cavities. This translational insertion is also a function of the pedicle screw. In the case of a screw, this is done by rotation that is converted into a translation, but a direct translation is also an option. This function is highly dependent on the types of fixation and perforation methods chosen, but all options boil down to only two fundamental options: Push-in insertion (translation) and screw-in insertion (rotation into translation).

1.3.4. Rigid connection and force transfer: Supportive function

The above functions do not yet lead to an integrated system: the separate functions still have to be rigidly connected. The pedicle screw should be able to withstand great forces and therefore a rigid connection between the anchor and the application point of the forces, the correction rod connection point, should be created. This rigid connection should be designed in a way to support the other functions and meet the strength requirements and is therefore considered later.

1.3.5. Connection point for correction rods or plates: Supportive function

These pedicle screws will together with rods or plates be used to create a rigid construct for spinal corrective surgeries. This means that there should be a rigid connection between the rods or plates and the screw itself. Most of the time the correction rods are clamped in a slot at this distal end by a small stump screw. This study only focuses on improving the fixation of the pedicle screw in the cortical pedicle. Therefore, the connection point to the rods or plates is not discussed and lies outside the scope of this project.

1.4. Target pedicle model

1.4.1. Choice for L1 vertebra

There are multiple papers reviewing the effects of different insert trajectories, screw augmentation, and Bone Mineral Density (BMD) on screw loosening. However, there is limited research done into whether screw loosening is more common in certain vertebrae than others. Murray [25] concludes that most cases of

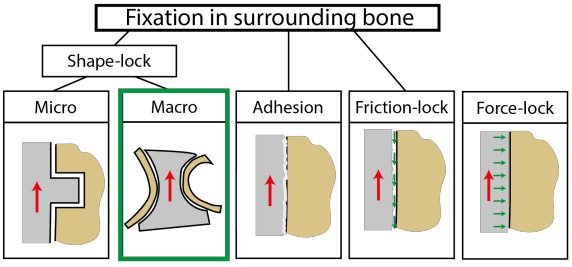

Figure 1.6: *Overview of possible fixation methods in bone*

screw loosening occur near the thoracolumbar and lumbosacral junction, which are respectively the transition region between the lumbar and thoracic spine (T11-L1) and between the lumbar and sacral spine (L5-S1). The highest rate of loosening occurred in the lumbar spine (10 out of 18 patients). To ensure that the solution applies to all affected vertebrae in the lumbar region, we take the vertebra with the smallest pedicle from this region as the basis for our model. The L1 vertebra has the smallest transverse diameter of the lumbar vertebrae and will thus serve as a target model. Although we set up a pedicle model as a guideline for designing the in-pedicle anchor, a design should always be able to fixate in pedicles with other dimensions within a certain range.

1.4.2. Simplified pedicle model

Before designing the in-pedicle anchor an environment model is created of the target pedicle. This model should be made in such a way that the model is a realistic representation of the real pedicle with some simplifications where needed. The complex internal shape of the pedicle cannot be translated into a model easily. The choice was made to reduce the pedicle model to a cortical block with an oval-shaped tunnel filled with cancellous bone that is defined by three different cross-sections: one at the pedicle isthmus and two at the ends of the tunnel. Another tunnel with a constant oval cross-section through the middle allows concepts to be directly inserted. This increases the creative freedom by allowing concepts that are not able to pierce cancellous bone axially. In a clinal application, this tunnel can be created by drilling two half-overlapping holes using a 5.5mm drill or tap. This tunnel will mostly remove cancellous bone, but also a small portion of cortical bone at the pedicle isthmus. This results in the cross-section at the pedicle isthmus that is displayed in Figure 1.7a. The exact way this model is made and what assumptions are made is described in Appendix A. The final model is depicted in Figure 1.7b as well.

1.5. Project Goal

Goal:

Design an in-pedicle anchor that increases the number of contact points between the anchor and the pedicle compared to a conventional pedicle screw to reduce toggling.

Subgoals:

- Create an in-pedicle anchor that after installation can transfer corrective forces
- Use an expansion mechanism to adapt the macro shape of the in-pedicle anchor to the internal shape of the pedicle cortex

1.6. Structure of the Report

This thesis starts in Chapter 2 with the setting up of the functional and geometrical requirements for a working in-pedicle anchor and wishes for the design. As a start of the systematic design approach, different expansion methods are categorized in a tree diagram in Chapter 3. The best resulting categories are selected and different concepts are generated for these categories. From these concepts, one concept is chosen to be further developed. In Chapter 4 the working principle and manufacturing of this final prototype are described. To validate this proof-of-principle prototype it is subjected to multiple experiments in Chapter 5 of which the results are presented in Chapter 6. Towards the end of the report, the main findings and limitations are discussed in the discussion in Chapter 7. The report ends with the conclusion in Chapter 8.

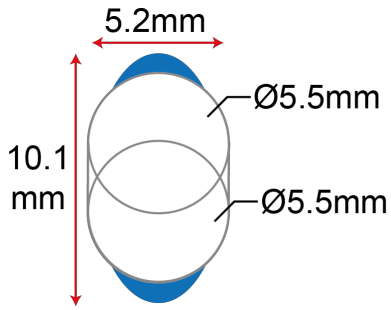

(a) *The dimensions of the pedicle isthmus.*

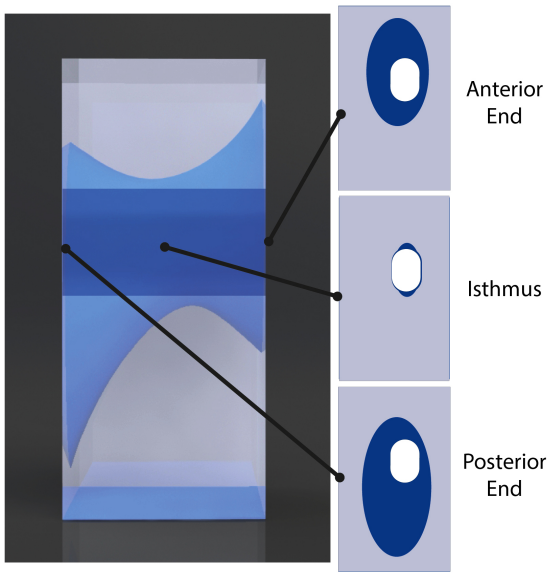

(b) *3D model of the pedicle including the cross-sections at the pedicle isthmus and both ends of the pedicle.*

Figure 1.7: *The simplified pedicle model*

2. Requirements

2.1. Functional requirements

The functional requirements describe the conditions that a design must meet. They are derived from the project goal and serve as a guideline for the design. They are also used for evaluating designs at different stages in the project. Because this is only a proof-of-principle design, requirements that only apply to clinical applications are left out.

1. No full penetration of pedicle cortex

The in-pedicle anchor has to fixate inside the pedicle and cannot perforate the pedicle cortex fully in any way. The anchor may partly penetrate the bone to achieve a better fixation, but there should not be a through-hole in the pedicle. This is to reduce the risk of damaging surrounding spinal nerves that lie around the vertebrae or the spinal cord inside the vertebral foramen.

2. Rigid after placement

The in-pedicle anchor should be able to transfer the correction forces from the connection point of the attached correction rod to the bone, which requires a fully rigid connection. Next to this, all (micro)movement of bone-contacting components is detrimental to the fixation of the in-pedicle anchor and therefore should also be avoided. This includes bending of components of the in-pedicle anchor, but also internal play between the components.

3. Accommodate for different patient sizes

Although the in-pedicle anchor will be designed for one specific pedicle model, the model should be scaleable in a similar amount of variants as conventional pedicle screws are. Pedicle screws generally use a sizing system with a minimum diameter of 4mm to a maximum diameter of 8 mm with increments of 0.5mm (9 variants). The system cannot be custom-made to fit the exact geometry of a patient's pedicle, so each in-pedicle anchor size must suffice for a small range of pedicle sizes and shapes within the sizing system.

4. No loose parts

Parts that can come loose from the in-pedicle anchor can lead to dangerous complications if not removed. If the design requires separate parts that are not permanently fixated to the in-pedicle anchor, there should be no possible way for these parts to come loose from the in-pedicle anchor and remain in the body even if the in-pedicle anchor fails or breaks.

2.2. Geometric requirements

From the simplified pedicle model described in Section 1.4 of the right L1 pedicle two main geometrical requirements can be derived that each concept should meet:

1. Should fit through the pedicle isthmus

To make sure that the in-pedicle anchor can be installed in the pedicle it should be able to fit through the smallest part of the pedicle; the pedicle isthmus. The isthmus of our model is displayed in Figure 1.7a and the cross-sectional dimensions during insertion should be kept smaller than these dimensions.

2. An expansion of at least 1.5x

Both the horizontal and vertical dimensions of the cross-section at the pedicle isthmus are between 2 and 2.5 times smaller than the cross-sectional dimensions at both ends of the pedicle model. To accurately mimic this shape, the dimensions of the ends of the installed in-pedicle anchor would ideally be 2 to 2.5 times as big as the dimensions at the center. To ensure a proper fit in the central region of the pedicle this ratio should be at least 1.5.

2.3. Wishes

Because this is an exploratory study, there are also conditions that the ideal in-pedicle anchor should meet, but limit the creative freedom too much or make the project too large to set as a requirement. These wishes are therefore not always quantifiable. However, these wishes are listed here and will be considered during the design phase of this proof-of-principle study and can help in a possible later practical implementation.

1. Expansion in two actions and vice versa.

To reduce the time it takes for the surgeon to deploy the in-pedicle anchor, the in-pedicle anchor should be easy to deploy. This means that a maximum of two actions is required before the in-pedicle anchor is fixated.

2. Improve contact with pedicle cortex

The current small contact area between the pedicle screw and the pedicle cortex should be improved in a new in-pedicle anchor. Increasing the amount of contact points can distribute toggling forces over more bone area and increasing the contact length can improve the toggling behavior of the in-pedicle anchor compared to the local centered cortical contact of a conventional pedicle screw. Assuming the two or three screw contact points described by Verdult [26] and a standard pitch of 2 mm, this results in a contact length of approximately 5 mm. The wish is to improve these both aspects of the pedicle cortex contact.

3. Resistant to toggling

The goal of adapting the macro shape of the in-pedicle anchor to the pedicle cortex and improving the contact area between the two is to make the in-pedicle anchor more resistant to toggling. This means that the final design should be significantly more resistant to (cyclical) lateral forces that represent physiological loading than a conventional pedicle screw.

4. Should compress cancellous bone

Before the in-pedicle anchor can adapt its shape to the surrounding cortical bone the cancellous bone inside the pedicle should be either removed, compressed, or pierced to let the in-pedicle anchor adjust its shape to the shape of the pedicle cortex. When compression of the cancellous bone is used, therefore, the bone should be compressed to a point where the cancellous bone has no significant influence on the rigid connection between in-pedicle anchor and pedicle cortex.

3. Conceptual Design of the In-Pedicle Anchor

3.1. Categorization of Expansion Working Principles

As one of the first steps in the design process, a categorized overview was created of all possible anchoring methods. Solutions for an in-pedicle anchor can be categorized in a lot of different ways: based on their movement, flexibility, shape, or other properties. The choice was made to categorize all possible expanding in-pedicle anchors in two levels: firstly based on their expansion movement and secondly based on their extender type. This overview including the two categorization layers can be seen in Figure 3.1.

The first categorization of all possible solutions is based on their expansion movement. These different movement categories form the first layer of our categorization and are depicted in the top row of Figure 3.1. The directions of these movements can give insight into whether an expansion is useful for adapting the macro shape of the anchor to the pedicle cortex. The expansion movement should be in the right direction to adapt its shape to the pedicle and the expansion direction should not make the anchor vulnerable to any unwanted flexibilities or movements. Four basic movements describe useful expansion movements for an in-pedicle expanding anchor: transversal rotation, axial rotation, radial translation, axial translation causing radial translation, and axial rotation causing radial translation.

Expansion methods that create a larger cavity than their final footprint remove more cancellous bone than necessary. This could influence the initial stability of the anchor. The first two categories, axial and transversal, rotation are examples of this. Moreover, the shape of the pedicle makes axial rotation undesirable, as this would mean that the pedicle cortex must be pierced to allow an extender to reach the top and bottom extremities of the pedicle. This goes against the requirement of not protruding the cortical bone. Transversal rotation requires extenders with a small frontal surface to pierce the cancellous bone. This small surface is undesirable because it makes the design vulnerable to rotation or toggling in the direction these extenders expand. These vulnerabilities make the axial and transversal rotation categories unsuitable for our application. The other three expansion movements expand and create a cavity that is fully occupied by the expanded anchor itself. This makes it less prone to undesirable movements such as toggling. Another benefit of these methods is that their movement is probably more easily reversed because there is no cavity that bone will grow back into. The extenders of the group that combines radial and axial translation do not fill the created cavity entirely, but the implementation determines whether this leads to a less stable system.

The second tier in the expansion method tree is divided based on the extender type. Both groups are named 'single points' and 'groups of points', respectively. This created overview gives insight into the rigidity of a certain method and the ability to adapt its shape accurately to the inner pedicle, which are both important features of the anchor. This overview can be seen in the second row of Figure 3.1. In this case, extenders are the outer moving components that adapt the shape of the anchor. These components can be either (part of) the main body of the anchor itself or a separate component that extends. Some methods have extenders that are fully independent of each other and therefore allow for larger differences in expansion lengths between adjacent extenders. Other methods have expansion parts that are linked to each other in some way. This makes their expansion lengths dependent on each other and limits the change in expansion between neighboring extenders.

3.2. Selection of Expansion Working Principles

3.2.1. Assessment requirements

Each method must at least meet three requirements to be a functional method: the anchor should be rigid after installation, should be able to perforate or compress bone and mimic the internal shape of the pedicle as accurately as possible. Without these three requirements, the new anchor will most probably not be more resistant to toggling compared to the standard pedicle screw. These requirements are deducted from the functional requirements and wishes from Chapter

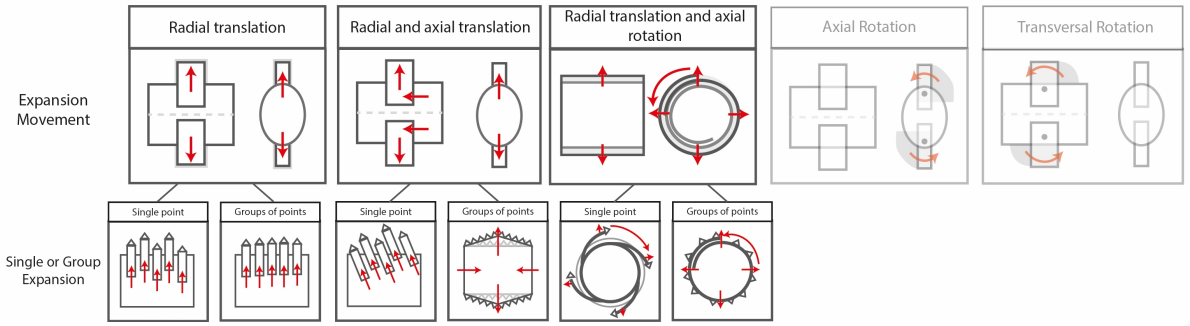

Figure 3.1: *Idea tree for expansion methods of a shape adapting in-pedicle anchor. The red arrows indicate the expansion direction of the different expansion methods. The expansion methods that are not suitable for our application are greyed out.*

2 and include the perforation and fixation features that an anchor must contain to be functional.

Rigid after placement

The different groups of expansion methods must have the potential to be rigid after placement in the pedicle. This means that the correction forces must be transferred from the distal end of the anchor to the bone-anchor interface without allowing (micro)movement. Therefore, the parts of the anchor should be rigid, but there should also be as little play as possible between the different parts.

Should compress cancellous bone

The pedicle still contains a layer of cancellous bone when the anchor can be placed. The anchor must pierce the cancellous bone layer to reach the cortical bone layer of the pedicle. The cancellous bone can also be compressed to a certain extent but this does not provide the stability that is required for rigid fixation. Both options could increase the stability of the in-pedicle anchor, which makes perforation of compression of the cancellous bone layer a requirement.

Improve contact with pedicle cortex

To reduce the amount of toggling the internal shape of the pedicle cortex should be followed as accurately as possible. There is a limitation to how accurate this can be, but there should be enough contact points with the pedicle cortex to provide more stability than conventional pedicle screws do.

3.2.2. Rating of Categories

All expansion methods are assessed on whether they meet the requirements and are given the score 'acceptable' or 'not acceptable'. Sometimes it is not clear whether a requirement is met or the score is highly dependent on the implementation of the method. Then the method is given the score 'unclear'. A method is rejected when one or more requirements have received a 'not acceptable' score. The scores and the final verdict are summarized in Figure 3.2.

Rigid after placement

Methods that make use of a radial translation and axial rotation, are mostly based on the flexibility of the material. Examples are methods that unwrap like a clock spring (Cat. 6) or flexible extenders that protrude through the main body through rotation (Cat. 5). This non-rigidity is used for the expansion of the implant, allowing it to adapt to the surrounding bone. However, this flexibility is a clear drawback after expansion. Even if reinforcements can be devised, there will always be some flexibility in the material, which prevents the corrective forces from being sufficiently transmitted from the corrective rod to the bone surface. The rigidity of methods that are based on rigid extenders for their extension (cat. 1 and 3) are mostly dependent on the dimensions of these extenders. Extenders with small cross-sections would introduce flexibility, hence the score 'unclear'.

Should compress cancellous bone

Whether a method can perforate the cancellous bone is dependent on multiple factors: the size and shape of the extenders' contact surface with the bone, the rigidity of the extender, and the force that can be generated. This makes it a hard requirement to assess resulting in an 'unclear' score for most methods. Single rigid points should be able to pierce the bone if the cross-section is made neither too small nor too large, so their score is established as acceptable.

Improve contact with pedicle cortex

There are two ways to mimic the shape of the pedicle and thereby increase the contact area between the pedicle cortex and the in-pedicle anchor: flexibility or multiple individual extenders. The flexibility of larger surfaces can be used to adapt the shape to the surrounding bones. Multiple extenders can be used to adapt the macro shape of the anchor with discrete expanded points. All methods that use groups of points instead of individual points are less suitable for mimicking the internal shape of the pedicle. There are fewer

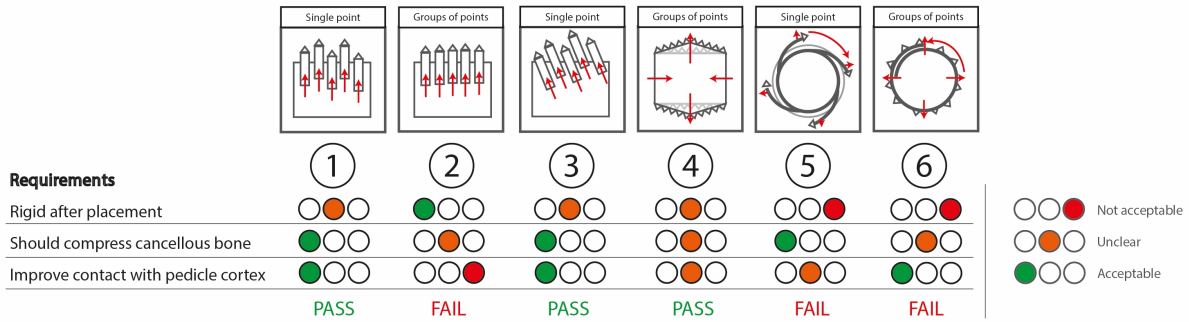

Figure 3.2: *Requirements and their score for different categories of expansion methods.*

points which makes the 'resolution' of the shape lower and the shape therefore less accurate.

3.2.3. Final verdict

All scores on the different requirements are shown in Figure 3.2. This summary shows that categories 1, 3, and 4 are the most promising for the further design process. The two factors of rigidity and shape-adaptability seem to contradict often in the different expansion methods. The tradeoff between these two factors will be an important consideration in the further design process and the optimum between these should be found for the final design.

3.3. In-Pedicle Anchor Concept Generation

In the next step, a number of concepts were generated within the three winning categories from Section 3.2. The concepts that were the most representative of the expected benefits and drawbacks of each category were selected. For categories 1 and 3, this meant that concepts were selected that highlighted the use of rigid single points and, thereby, adapt its shape discrete to the pedicle cortex. For category 4 this meant that a concept was selected that used the benefit of having groups of points and flexibility to allow for a continuous adaptation to the shape of the pedicle cortex and thereby the most possible contact. The most promising concepts were selected for an evaluation based on the requirements and wishes. An overview of the selected concepts is shown in Figure 3.3. The corresponding categories for Concepts 1, 2, and 3 are categories 1, 3 and 4 respectively. Concept 1 originally had a housing that made the part of the extender that would extend beyond the confines of the anchor move in the radial direction. This is why the concept was placed in the radial translation category (Cat. 1). In practice, this turned out to be impossible due to the scale and the housing was removed from the design. The extenders in the eventual design translate radially and axially and therefore can better be placed in the corresponding category (Cat 3). The 3D models of the three concepts and their prototypes after expansion during an experiment are depicted in Figure 3.4.

3.3.1. Concept 1: Stars

This concept is based on a conical expansion piece with protrusions giving it a star shape as shown in Figure 3.4. Due to the conical shape of the expansion piece, these protrusions will expand when compressed by the base of the next expansion piece. These pieces are threaded on a bolt and a nut at the other end draws the expansion pieces towards each other. The theoretical working principle is that when the pedicle cortex is reached by one of the expansion pieces the expansion stops due to the resistance of the pedicle cortex. Other expansion pieces that have not reached the cortical bone can still expand by moving toward each other. This allows the total shape to adapt to the pedicle cortex.

3.3.2. Concept 2: Wedges

The wedges concept is rigidity-based: it consists of rigid components that can move with respect to each other and thereby change the macro shape of the anchor. Because of the rigid parts, the main challenge is not the rigidity of the concept prototype, but achieving an accurate adaptation of the shape to the pedicle cortex. Multi-stage expansions are very fragile at this scale, so the choice was made to keep a one-stage expansion. This, however, limits the maximum expansion of the anchor. The concept prototype consists of a central bolt and six wedges. The expansion is caused by the slanted surface on these expansion wedges. For this concept prototype, the choice was made to expand in both vertical and horizontal directions. The wedges, therefore, have two slanted sides that are vertically oriented on one side and horizontally on the other (Figure 3.4). The inclination angle of the wedges is both in vertical and horizontal direction 25°. A central slot allows the wedges to be threaded on a bolt and to move with respect to each other. When the nut is screwed on the bolt and the wedges are drawn towards each other the wedges will expand in the direction that the slots and wedges allow. If one wedge

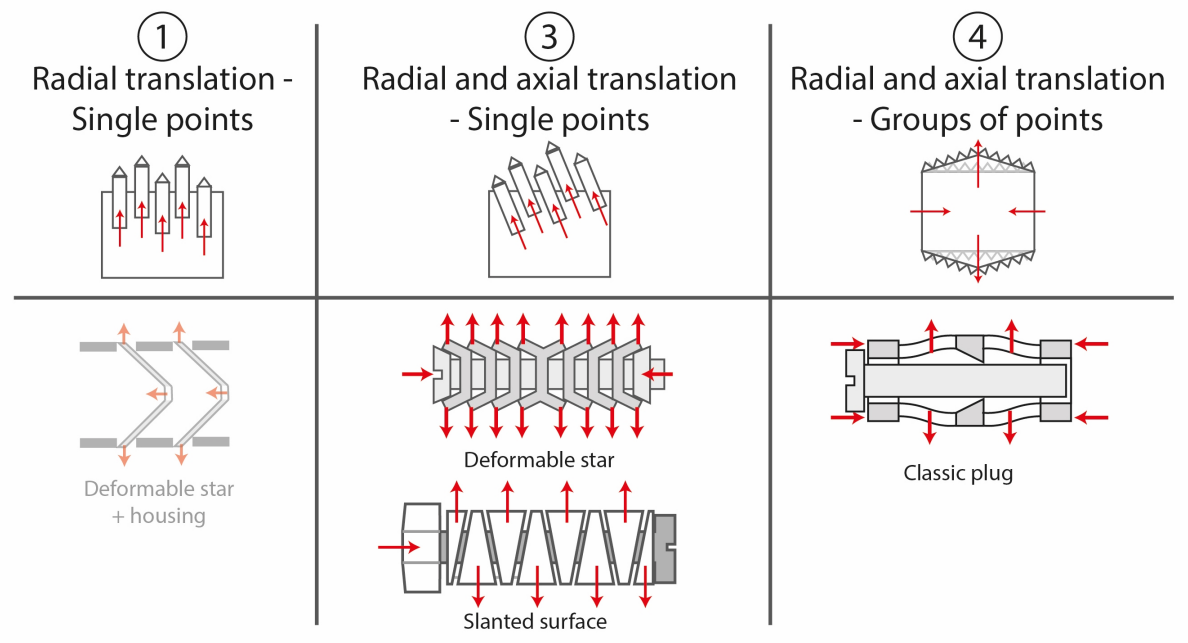

Figure 3.3: *Overview of the selected generated concepts and their corresponding categories.*

reaches the cortical bone the other wedges can still expand further. As a result, the total footprint of the anchor will adapt its shape to the inside of the pedicle. The expansion wedges can have a cross-section that is a fraction smaller than the isthmus.

3.3.3. Concept 3: Plug

The third concept is based on a classic plug that is used to fixate something in a wall. This similarity is visible in Figure 3.4c. This is a flexibility-based concept: it makes use of flexible components to change the macro shape of the anchor. The challenge here is to use flexible components and still achieve a rigid solution. Two round-end pieces are connected by multiple long rectangular strips. To expand the anchor a bolt is inserted through both end pieces and the center of the anchor. On the other side, a nut is screwed on the bolt. When the bolt is turned with respect to the nut the two end pieces will move towards each other and thereby bend and expand the multiple strips. Internal protrusions will ensure that the expansion of the strips happens outwards.

3.4. Selection of In-Pedicle Anchor Concepts

3.4.1. Toggling Experiment

The three concepts from Section 3.3 were all 3D printed out of Tough 1500 resin using a Formlabs Form 3. The thickness of the flexible parts in Prototypes 1 and 3 has a big influence on the shape-adaptability and rigidity of the concept prototypes and, therefore, on their toggling behavior. The thicknesses of these parts were kept equal to factor out this variable.

An experiment was done to compare the different concept prototypes quantitatively. Due to the sample size, no exact conclusions can be made, but it can give an indication of the performance and at the same time observe potential problems in the designs. The detailed experiment protocol, pictures, and results are found in Appendix B. The goal of the experiment was to show the difference in lateral stiffness between the different concept prototypes when installed in a pedicle model and subjected to a lateral force. This property is important because it gives a quantitative measurement of the resistance to toggling which is a combination of the rigidity of the concept prototype combined with the ability to adapt to the shape of the internal pedicle.

This experiment can also give an insight into whether rigidity of the concept prototype or exactly following the pedicle cortex shape should have priority in the trade-off between rigidity and ability to adapt the shape and thus whether flexibility-based concepts (Prototype 1&3) or rigidity-based concepts (Prototype 2) perform better. During the experiment, the displacement angle of the prototypes and the input force causing this displacement were measured. This would result in a graph like the one depicted in Figure 3.5 From this graph the input force at the 0.5-degree displacement threshold can be determined, shown by the yellow line and orange star. These forces at 0.5-degree displacement are summarized in Table 3.1.

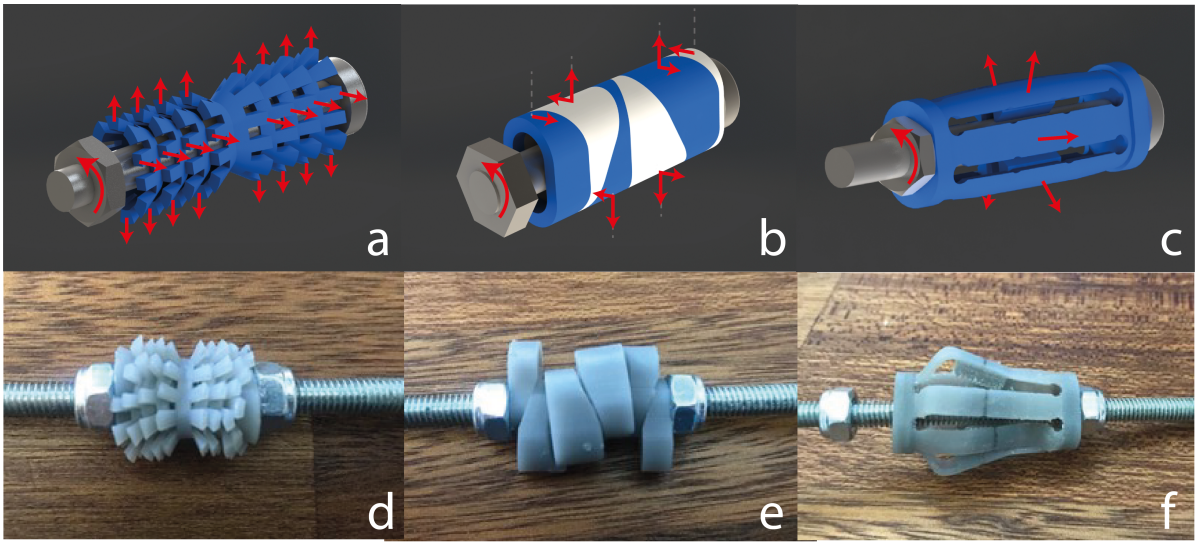

Figure 3.4: *The three concept prototypes. a) Star principle - 3D Model. b) Wedges principle - 3D Model. c) Plug principle - 3D Model. d) Star principle - Concept Prototype after experiment. e) Wedges principle - Concept Prototype after experiment. f) Plug principle - Concept Prototype after experiment.*

Table 3.1: *Measured forces at the 0.5 degrees threshold.*

	1: Star	2: Wedges	3: Plug
Cranial	7.31 N	3.89 N	3.86 N
Caudal	9.99 N	11.02 N	4.17 N

3.4.2. Concept Selection

The data from the experiment shows that the plug is the least stiff concept prototype of the three. This can be explained by the long flexible parts. These results were confirmed by inspecting the plug concept prototype after the experiment (see Figure 3.4). The plug concept prototype was completely deformed due to the lateral loads. Moreover, the plug concept prototype was heavily twisted due to the rotation friction induced by the nut, even when a washer was used. The star prototype shows that many flexible parts that are compressed can result in a relatively rigid system. It almost matches the results of the wedge concept prototype in the caudal direction and is stiffer in the cranial direction. The photos of the star concept prototype in Figure 3.4d show that the small protrusions require great deformations to fixate in the model. However, the great stresses that would occur in a metal

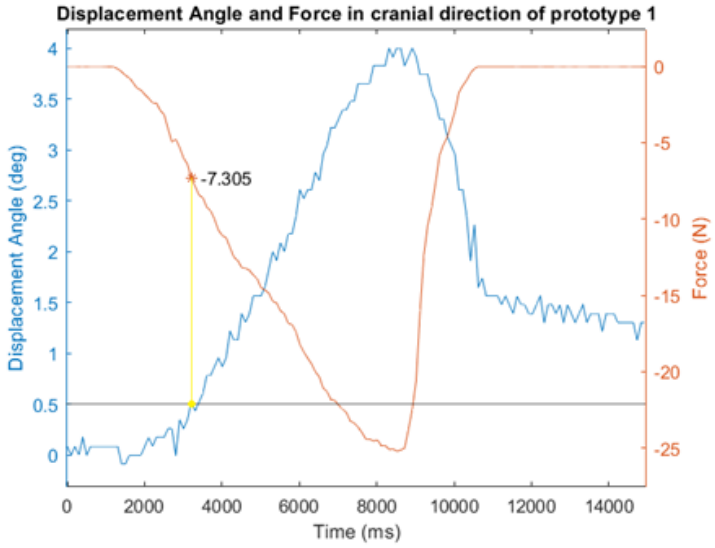

Figure 3.5: *Force-displacement graph of a lateral stiffness measurement for Prototype 1. The orange star indicates the force at the 0.5 degree threshold (black line).*

variant combined with these small protrusions may result in small parts becoming detached. This can lead to dangerous situations when implanted in the body and thereby violates the set requirements.

Although all three concept prototypes can be improved a lot, the wedge concept prototype seems the most promising for further development. Possible improvements for the wedge concept prototype lie in achieving a controlled expansion. During the experiment each wedge can move in the vertical and horizontal directions at the same time, making the whole expansion unpredictable and messy. This phenomenon is visible in the photo made after the experiment in Figure 3.4. In addition, the wedges can rotate around the round central screw, which makes this effect even worse. It is also striking that this wedge concept prototype works much better in the caudal direction than the cranial direction. This could be caused by the chaotic unfolding, but this difference is most probably caused by the asymmetrical shape of the internal pedicle. This may not be a problem, because the greatest forces in the back are in the caudal direction [27], but sufficient support also should be provided in the cranial direction.

4. Detailed Design of the Final In-Pedicle Anchor Prototype

4.1. Working Principle of the In-Pedicle Anchor Prototype

This final proof-of-principle prototype is based on one of the classical simple machines: the wedge. The wedge can be used to transfer forces and change their direction. An input clamping force can be transformed into an output expansion force in the perpendicular direction. The compressive force induced by the nut will cause a normal force perpendicular to the sliding surface. In this clinical application, these normal forces must overcome the resulting friction forces and the resistance force of the cancellous bone to expand the proof-of-principle prototype. An illustration of these forces on the wedges can be seen in Figure 4.1.

The surface that will compress the cancellous bone can be changed by, for example, adding spikes or cutting edges. This will possibly ease the unfolding of the proof-of-principle prototype by applying more of a shear load than pure compression and thereby cutting through the bone. However, to create a baseline proof-of-principle prototype, it was decided not to pay attention to this variable and to use a flat surface that will compress the cancellous bone. It is important that on either side of the bolt there should be a contact point between the main bolt and an expansion wedge, which should be the case as shown in Figure 4.2. This combined with the clamping pressure of the nut and bolt ensures that the bolt can transfer a load from the attachment point to the cortex without rotating in the central tunnel of all the wedges. Whether the proof-of-principle prototype will work is highly dependent on the chosen inclination angle of the wedges. When a larger inclination angle is chosen the normal force is more directed upwards. This decreases the required input compression force, which in turn decreases the friction forces that should be overcome. However, a larger inclination angle also enlarges the contact area with the cancellous bone. This means that more cancellous bone must be compressed to allow the wedges to expand. These two counteracting phenomena were modeled in the next section to provide an insight into what inclination angle is suitable for our application.

4.2. Theoretical Friction Analysis

In MATLAB a model was made of the required compression force to compress 17 PCF Sawbones solidbone foam. The friction forces between the wedges are highly dependent on the Coefficient of Friction (CoF) of the wedges and, therefore, depend on the materials and their surface finish. Because it is hard to estimate

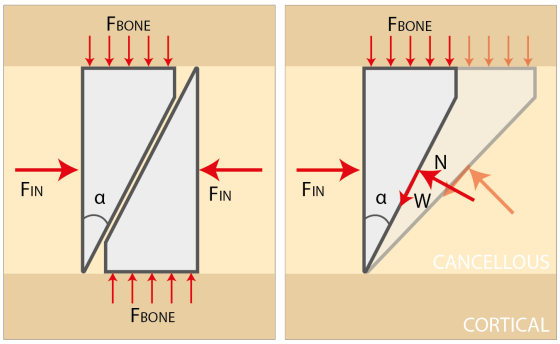

Figure 4.1: *Depiction of the forces on the expansion wedges*

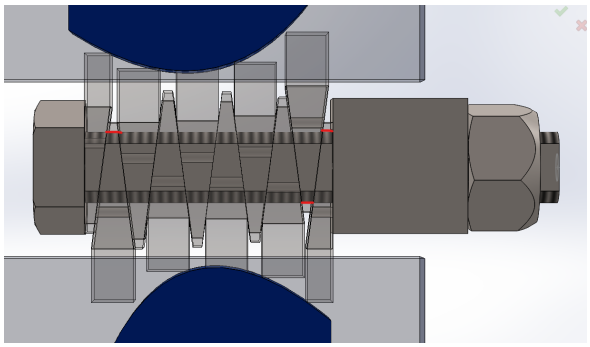

Figure 4.2: *The prototype expanded in the pedicle model in SolidWorks. The three red lines indicate a contact point of the bolt with the wedge*

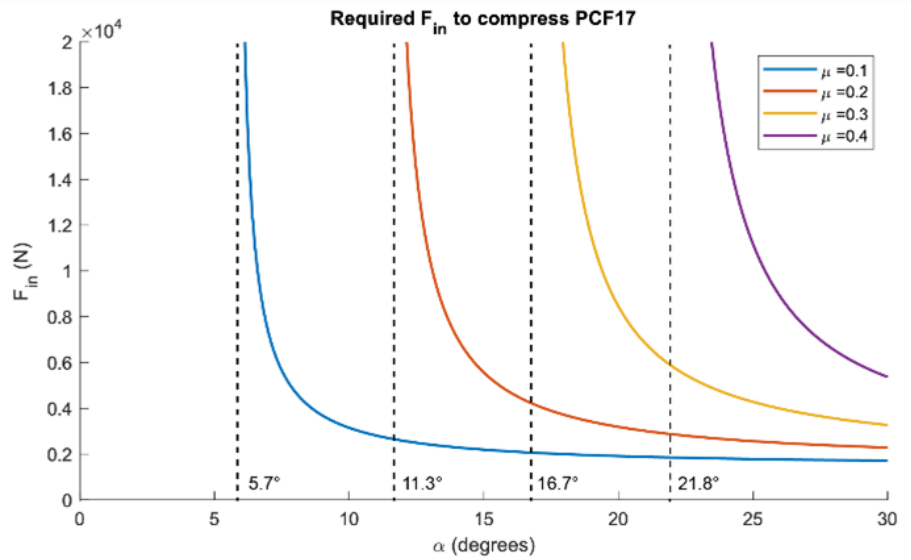

Figure 4.3: *Graph of the required input force to compress 17pcf Sawbones bone foam including the friction asymptotes*

an exact CoF, four different levels of CoF were used to calculate the required input compression force for all inclination angles. The resulting graph is shown in Figure 4.3. This graph also shows four asymptotes that indicate the minimum angle before self-locking appears. Self-locking is a phenomenon that two surfaces will not move with respect to each other independent of the input force because the friction force is too large. A system of two wedges is self-locking if:

$$\mu > tan(\alpha) \tag{4.1}$$

If the minimum angles are calculated with Equation 4.1 for the four different CoFs they match the asymptotes of the modeled input force graphs. In Figure 4.3 the asymptote representing the minimum angle for each given CoF can be seen.

From this model, we can derive that we should have an inclination angle for a certain CoF that is not below the self-locking angle, but also not close to it. An inclination angle that is too close to the minimum angle can lead to high required input forces. This makes the choice for a certain inclination angle a trade-off between the number of wedges, which improves the resolution, and the required input force. To determine the most favorable inclination angle the CoF of the used material should be known.

This value is unfortunately difficult to determine because the proof-of-principle prototype will be made from stainless steel. This material is surrounded by a microscopically thin chromium oxide layer which forms when the chromium in the stainless steel reacts with the oxygen in the surrounding air. This layer not only protects the material from corrosion but also improves its frictional properties. This regenerative oxide layer, which is only a few nanometers thick, separates the two metal surfaces. However when high surface pressures are applied, the oxide film will be pierced and the bare metal surfaces will touch, increasing the friction [28]. There are no exact values at what surface pressure this breakdown happens, but in our application, the surface pressures are relatively small due to the larger sliding surface compared to surface pressures that occur in for example stainless steel bolt-nut connections (30-100x smaller). The exact calculation of these surface pressures is done in Appendix C.4. This low surface pressure makes a CoF of 0.22 for martensitic hardened stainless steel provided by the British Stainless Steel Association (BSSA) most likely not accurate for our application in the lower density bone foams [29].

Without an indication of the CoF of the material, there is no way to know whether the chosen inclination angle is close to the minimum inclination angle. Therefore, the choice for an inclination angle of 7.5° was based purely on the resolution it would provide. This angle allows for the use of ten wedges, eight middle and two end wedges, in the length of the pedicle. This seems like a minimal sufficient resolution to mimic the internal pedicle cortex shape accurately. The number of wedges with an inclination angle of 7.5° that fitted in the pedicle was established by fitting the expanded proof-of-principle prototype model in the pedicle model in SolidWorks. This process is displayed in Figure 4.4.

4.3. Final Prototype Design

4.3.1. 2D Simplification of Prototype

The goal of this project was to design an in-pedicle anchor that minimizes toggling. This toggling is more apparent in the caudocranial direction than in the

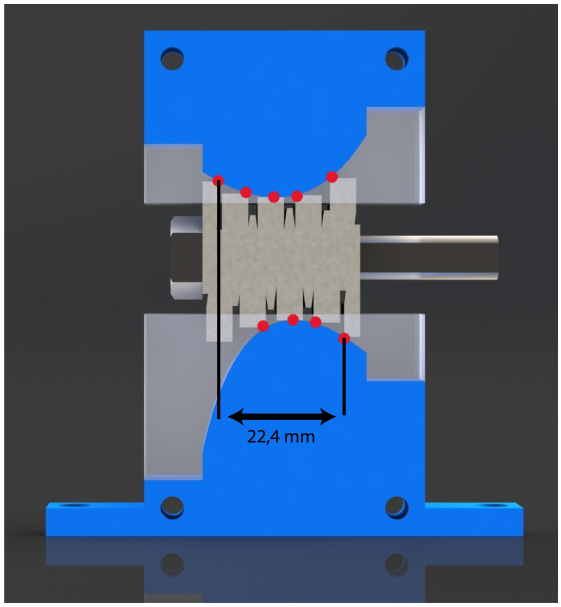

Figure 4.4: *Visualization how the maximum amount of wedges that fit in the pedicle model in expanded state are determined. The theoretical maximum contact length is also determined.*

medial-lateral direction due to higher loading. The needed expansion in the vertical direction is also larger than in the horizontal direction due to the asymmetric anatomy. Because of this, the choice was made to simplify the proof-of-concept prototype to a two-dimensional (2D) model that can expand in the caudocranial direction. A simplified 2D model shows the working principle and keeps one dimension free for observing the exact movement of the expansion and adding potential supporting functions. Next to these advantages, one extra advantage of this simplification is that the described problem of a chaotic expansion of the first 3D printed concept prototype in Section 3.3 was no issue in this prototype due to the 2D expansion. It is possible to translate this design back to 3D and there are multiple options to do so. An adaptation of a conventional pedicle screw or a system fully based on expansion are both an option. In such a future 3D implementation the contact area in the transverse plane between the in-pedicle anchor and the pedicle cortex should be kept in mind. To increase the ease of making visual observations and simplifying the fabrication the proof-of-principle prototype was scaled up to 200%.

The design of the proof-of-principle prototype prototype and pedicle model went hand in hand. The polylines that are described in Section 1.4.2 are extruded to create a 2D profile of the cortical pedicle. The same assumption is made that, in clinical use, a tunnel in the cancellous bone is made. This 3D oval tunnel of the first pedicle model was translated to a rectangular tunnel in the 2D model as can be seen in Figure 4.5. The thickness of the cortical walls of the pedicle is again not taken into account and the internal pedicle model is designed in a solid rectangular block. The dimensions of the sagittal cross-section are kept the same as the 3D simplified pedicle model. The proof-of-principle prototype was simplified into a 2D model by making the wedges rectangular in the same way as the tunnel.

4.3.2. Manufacturing of Prototype

All parts of the final prototype are fully made from stainless steel (316L). The ten sliding wedges are manufactured through Electrical Discharge Machining (EDM) and the central bolt is made from a stainless steel M8 bolt. The sides of the bolt are flattened with a mill to provide a guiding surface for the wedges during expansion. The thread on the top and bottom side of the bolt still allows a nut to be threaded on and engage with the weges. The central bolt has a length that slightly sticks out of the pedicle model. This allows for an easy application of the nut to the thread. To allow the use of a torque wrench with sockets for tightening the proof-of-principle prototype an extension tube was added to the design. This extension tube transmits the force from the nut to the first wedge. Each wedge, the extension tube, and the head of the bolt have two holes that all align and allow a small pin to be inserted to fixate the proof-of-principle prototype in the unfolded position. This allows the proof-of-principle prototype to be inserted in the pedicle without the wedges expanding and obstructing the insertion. The wedges at both ends of the prototype are slightly different from the middle wedges and have only one slanted surface. The other side is a straight vertical surface that increases the contact area with the extension tube or the head of the bolt to decrease local peak forces. All parts were deburred and polished in a barrel finishing machine to improve the frictional properties. The final prototype and its dimensions can be seen in Figure 4.6.

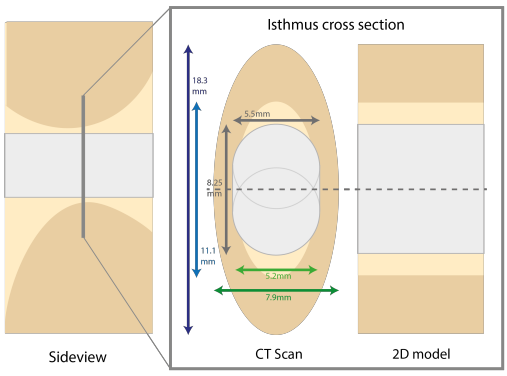

Figure 4.5: *2D simplified pedicle model*

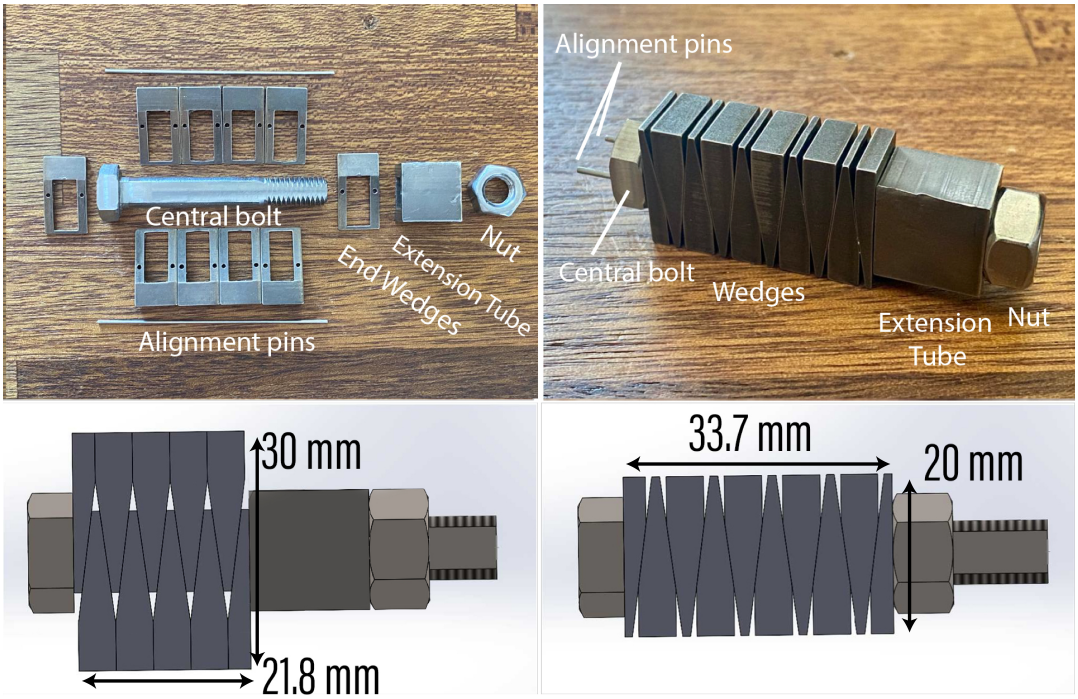

Figure 4.6: *Proof-of-principle Prototype Design. a) Photograph of the different components of the prototype with their description. b) Photograph of the assembled prototype. c) Side view of the prototype including dimensions (unexpanded state). d) Side view of the prototype including dimensions (expanded state).*

5. Experimental Validation of the In-Pedicle Anchor Prototype

5.1. Experiment 1: Cancellous Bone Compression

5.1.1. Experiment Goal

The goal of this experiment is to test whether the proof-of-principle prototype can compress cancellous bone and to find the relation between the input torque and the wedge displacement. This experiment will validate whether the system complies to Wish 4: "The total system should be able to remove, compress or pierce cancellous bone".

5.1.2. Experiment Variables

Independent Variables

Bone foam density

Cancellous bone can have different densities depending on the patient's age and the possible presence of osteoporosis. To test the feasibility of the proof-of-principle prototype for different target groups it is interesting to know whether the prototype can compress all possible densities of human cancellous bone. For this experiment, three different densities of Sawbones Solid Rigid Polyurethane Foam are used with the densities of 5, 10, and 15 Pounds per Cubic Foot (PCF). These foams are designed to mimic heavily osteoporotic, slightly osteoporotic, and healthy human cancellous bone respectively. The compressive strengths of these materials are 0.6, 2.2, and 4.9 MPa respectively [30]. The ultimate compressive strength of human cancellous bone is similar, but is highly dependent on age and can differ from 4.6 MPa at age 20 to 1.2 MPa at age 80 in the caudocranial direction [31].

Wrench input torque

The input torque on the compression nut was gradually increased in steps of 1Nm in the range of 1-14Nm. This input torque gives an indication of the effort that is required to expand the proof-of-principle prototype inside the cancellous bone.

Dependent Variables

Horizontal and vertical displacement of the wedges

The position of the ten wedges at each torque input shows how far the proof-of-principle prototype compresses the cancellous bone for a certain set of input torque. This not only shows the effort to fully expand the proof-of-principle prototype inside cancellous bone of different densities but also shows the different paths that the different wedges take to reach full expansion.

5.1.3. Experimental Facility

The experimental facility, shown in Figure 5.1, consists of a clamping system and an alignment block attached to a Thorlabs MB2530M breadboard. Two 3D-printed L-shaped clamping blocks (white) and four M5 bolts are used to clamp down on the PMMA to keep the Sawbones Solid Foam (beige) and proof-of-principle prototype in place and make sure the expansion of the prototype only happens in one plane. An alignment block (blue) is used to make sure that the prototype is placed between the two bone pieces at the same place and orientation every time. All 3D-printed parts were made on a Creality Ender 3 Pro using generic PLA. A 1.4" CXWXC torque wrench with a range of 1-25 Nm was used to apply the input torque for the expansion of the prototype. The accuracy of this wrench torque output is claimed to be +/- 4%. The photos were made using a Sony A6000 camera with a 35mm f/1.8 lens. The camera was mounted on a tripod facing straight downwards to minimize differences in perspective and scale between the different photos.

5.1.4. Experiment Protocol

Before the experiment was started a photo is taken of the starting position. Next, a torque of 1 Nm was applied using the torque wrench. At this point, another photo was taken. Now the torque was set to 2 Nm and the process was repeated. This procedure is repeated with increments of 1 Nm until two of the wedges were visually fully expanded or the maximum set torque of 14 Nm was reached. It is not always exactly clear whether the wedges have reached the maximum expansion, so to prevent damage to the prototype a maximum torque was set. This whole experiment was repeated three times for each bone density.

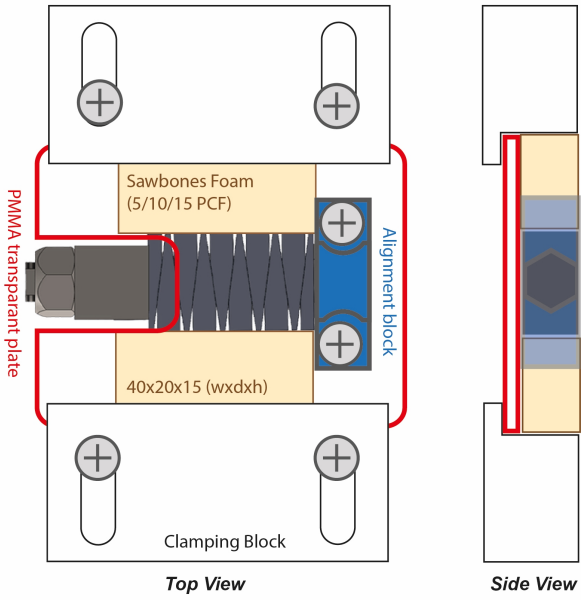

Figure 5.1: *Depiction of the experimental setup for the bone compression experiment.*

5.1.5. Data Analysis

The photos taken after each torque increment do not show the exact endpoint of each wedge due to the bone that blocks the view. To solve this, the photos were loaded into Adobe Photoshop to add the known outlines of the wedges. Although the camera was mounted on a tripod, not all the images were exactly aligned. In Photoshop two diagonal lines are drawn between the corners of the L-shaped brackets. The intersection of these two lines is assumed to be the center of the clamping system. This process can be seen in Figure 5.2a. The center of each photo is exactly aligned and each photo is rotated so that the prototype is oriented horizontally every time. This means that the tendency of the prototype to rotate is not visible in the data and only the horizontal and vertical displacement of each wedge was determined. The endpoints of the unexpanded prototype were displayed as an overlay over each photo. These points act as a reference point for a measurement of the displacement of each wedge.

Next, a custom script was used that allows the measurement of lengths in photos based on a reference scale. The first inputs are the reference scales length and a line in the photo indicating the reference scale. For each photo, the height of a wedge (20mm) was defined as the reference scale. After this, a measurement line can be drawn from the unexpanded starting position to the current wedge position for each of the ten wedges in the photo after which the displacements will be calculated (Figure 5.2b). The average and standard deviation of each of the three repetitions were calculated and plotted in the same graph as each measurement. To keep clear insightful graphs, some data points have been omitted. For the 5 PCF bone, the measuring points are shown in torque steps of 2 Nm and for the 10 PCF bone in steps of 3 Nm. The data analysis and generation of plots were performed with MATLAB R2021b.

5.2. Experiment 2: In-pedicle expansion and lateral loading

5.2.1. Experiment Goal

This experiment consists of two parts: the in-pedicle expansion measurement and the lateral load-displacement measurement. The goal of the first part is to show whether the prototype can adapt its shape to the surrounding pedicle cortex and to what extent the prototype expands, in the same way, every time. This experiment shows whether the surface area between the prototype and the pedicle cortex is increased compared to the conventional pedicle screw

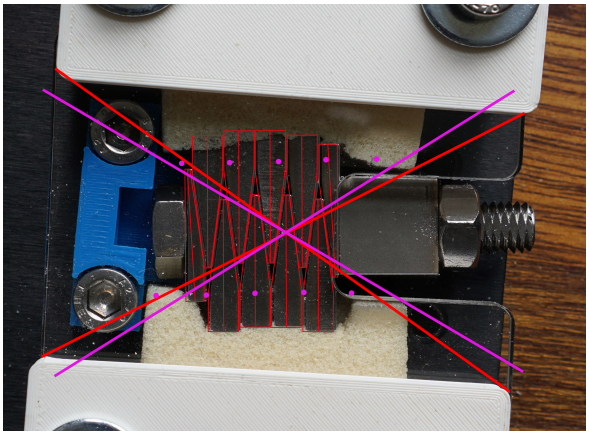

(a) *Picture of the test-setup during expansion with the crosses indicating the middle of the test set-up. The pink dots and cross indicate the end points and middle of the original unexpanded proof-of-principle prototype. In red the middle indication and outlines of the current expansion is shown.*

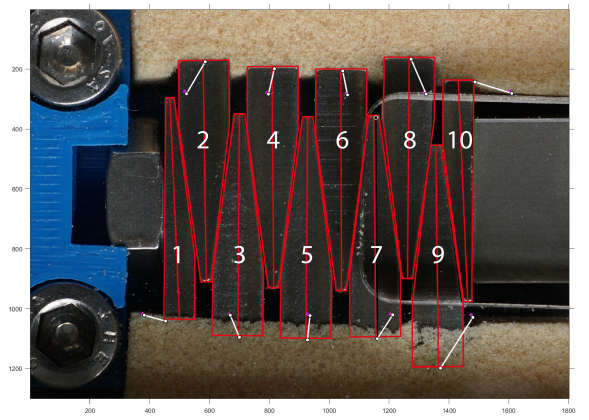

(b) *Depiction of how the expansion of each wedge is determined in MATLAB. The black line indicates the reference line, white the different measurement lines between start point (pink dots) and end point (middle of each red outline) of each wedge. The numbers indicate the wedge number.*

Figure 5.2: *Data collection from images of bone compression experiment*

(Wish 2). The second part of the experiment should be able to give an insight into whether the expansion of the 2D prototype helps prevent toggling (Wish 3). *In-vivo* pedicle anchors are subjected to complex loading conditions, but most studies simplify their experiments to cyclic lateral loading in the caudocranial direction. These loads require a complex setup with an actuator applying these cyclical loads. To keep the experiment as simple as possible the choice was made to do an angular displacement experiment by subjecting the prototype to a single non-cyclical lateral load.

5.2.2. Experimental Variables

Independent Variables

Prototypes

In this experiment, the earlier described prototype (section 4.3) and a mock-up model are used (Figure 5.3a). The mock-up model has the same shape and dimensions as the prototype in the unexpanded state. The experiment will be done with both to compare the resistance to toggling of a rigid, unexpanded mock-up model with the prototype in the expanded state.

Caudocranially applied force

In clinical use of in-pedicle anchors, according to Pinto *et al.* [32] the caudally directed loads (negative z-axis direction) are predominant. Therefore, the input force will be in the first place applied in the caudal direction. A load will also be applied in the cranial direction afterward, to see whether the prototype functions equally in both directions.

Dependent Variables

Contact points with the pedicle cortex

Both the number of contact points with the pedicle cortex and the distance between the two outermost contact points can give an indication of the stability of the prototype. A contact point is a point where the distance between a wedge and the pedicle cortex is a maximum of 1 mm. Real contact with the pedicle cortex is impossible because the Sawbones solid foam is compressed and not removed or pierced.

Angular displacement

The resulting angular displacement of the prototype compared to the mock-up model shows whether the prototype is more resistant to transverse loads than a rigid non-expanding prototype.

5.2.3. Experimental Facility

The experimental facility consists of a 2D pedicle model on two elevating pillars attached to an MB2530M breadboard. The pedicle model is based on the model described in Section 4.3 and is made from two 3D-printed PLA shapes that represent the pedicle cortex. A negative image of this shape made from 5PCF Sawbones bone foam represents the cancellous bone layer inside the pedicle and is attached to the pedicle cortex with double-sided tape. This foam was created by placing foam in a jig and filing away the excess foam (Figure 5.3b). The gap in between both cancellous bone pieces is the 2D representation of a drilled tunnel in the same way as the model in Section 4.3. Two bone pieces at the underside of the model are attached to support the weight of the prototype and the attached inclinometer. The breadboard is fixated to a stable surface to prevent the breadboard from moving by the applied forces. A drawing of the test setup is visible in Figure 5.4. The same 3D printer, torque wrench, and camera on a tripod were used as in Experiment 1 in Section 5.1. The displacement angle was measured using a Seika NG4i Inclinometer and the applied input force

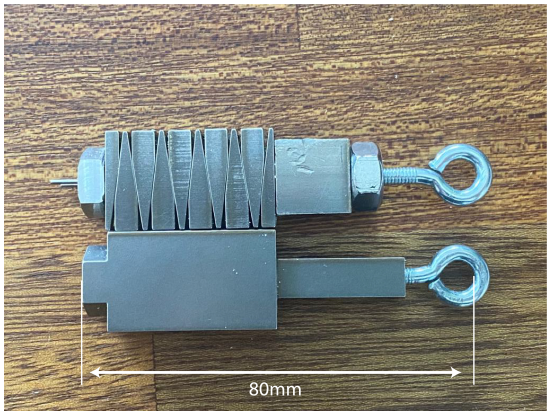

(a) *The prototype and mock-up model including their length.*

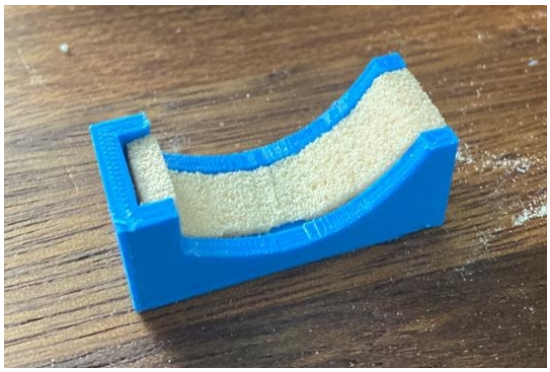

(b) *Image of how the Sawbones solid foam was filed to size using a jig.*

Figure 5.3: *Experiment 2: In-pedicle expansion and lateral loading preparation.*

was measured with a Futek 111N mini loadcell. A measurement amplifier (Scaime CPJ Rail) and DAQ device (NI USB-6008) were used to connect the sensors to a laptop running NI Labview 2018.

5.2.4. Experimental Protocol

Part 1: preparation and in-pedicle expansion

First, the inclinometer is secured to the head of the prototype by an M4 bolt. Next, the prototype is inserted between the two cancellous bone pieces in the central channel. The two PMMA plates are secured and the two supporting bone pieces are attached with double-sided tape. A photo is taken from the setup before the expansion. Next, the prototype is expanded by using the torque wrench until a resistance torque of 10 Nm is reached and another photo is taken of the expanded prototype.

Part 2: Lateral load-displacement measurement

After the prototype is fully clamped in the pedicle, the load cell is attached to the top of the prototype with an M3 screw eye to allow a caudal pulling force. The string is attached to the load cell and laid over the pulley, next a hook is attached to the other end of the string. In Labview, an offset is added to set both sensors at zero. After all these preparations were done, the video recording and measurement in NI Labview are started. The caudal force is slowly increased by adding weights to the hook in steps of 1 kg. Between each weight step, there was a ten seconds pause to give the system a chance to reach a steady state. After all 11 kg is added to the hook the measurement and recording are stopped. Next, the whole breadboard is rotated 180 degrees and the load cell is attached to the other side of the screw eye to allow a cranial pulling force. After the sensors are zeroed out again a new video and measurement are started and the measurement is repeated. The total experiment is repeated three times for both the prototype and mock-up model.

5.2.5. Data Analysis

The same custom script as in the compression experiment from Section 5.1 was used that allows the measurement of lengths in photos based on a reference scale. This data analysis and generation of plots were performed with MATLAB R2021b. The data out of NI Labview was converted to a Matlab input file. The time interval of the last stable two seconds in the force data was determined visually from the graphs. To filter the noise from the data, the average of the force and angle data for these intervals during each weight step were taken, as shown in Figure 5.5. The original raw data can be found in Appendix D. The photos made before each attempt were combined with a screenshot of the recording during maximum loading of the prototype. This alignment and the addition of the outlines happened in Adobe Photoshop.

6. Results

6.1. Experiment 1: Cancellous Bone Compression

The prototype expanded successfully in both 5 and 10 PCF solid foam in all three experiment attempts. To get a more visual context of the resulting expansion paths of these attempts an example visualization is made in Figure 6.1. This image shows the expansion path of the prototype wedges in the second experiment in 5 PCF solid foam. All of the resulting expansion paths of the wedges in 5 PCF and 10 PCF are depicted as a graph in Figure 6.2 and Figure 6.3 respectively. The prototype failed to expand in 15 PCF solid foam and created no more than a small indent in the material. As a result, the experiments in this solid foam density were stopped. It was experimentally shown that the wedges were able to successfully expand within 5 and 10 PCF Sawbones solid foam, which has similar properties to osteoporotic cancellous bone. Moreover, under lateral forces, the prototype rotates less in the designed pedicle model than an unexpanded solid mock-up model with the same dimensions.

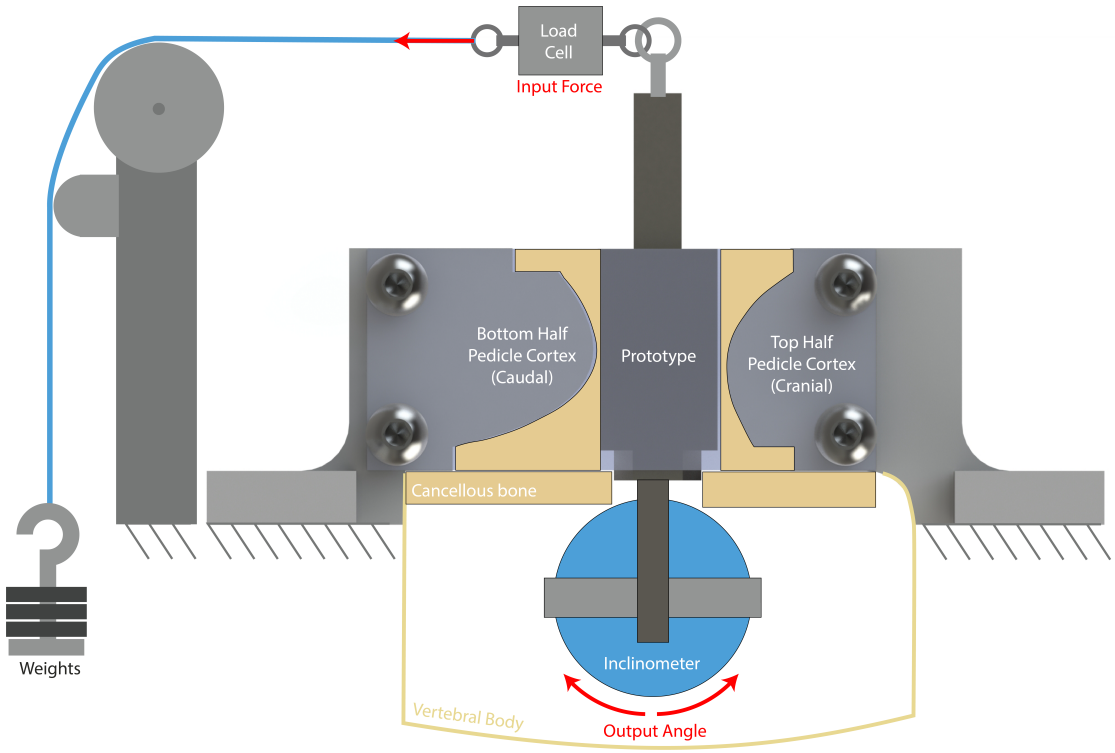

Figure 5.4: *Experimental Setup of Experiment 2: In-pedicle expansion and lateral loading.*

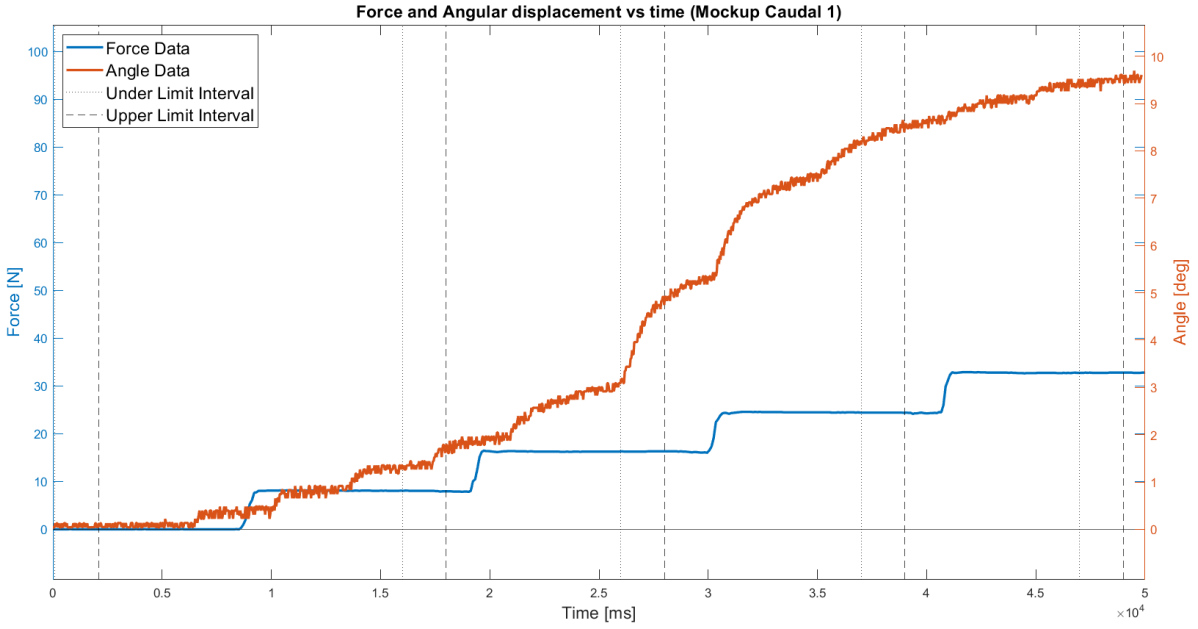

Figure 5.5: *Part of a measurement graph, from Experiment 2: In-pedicle expansion and lateral loading, showing the time intervals over which the average sensor data was taken.*

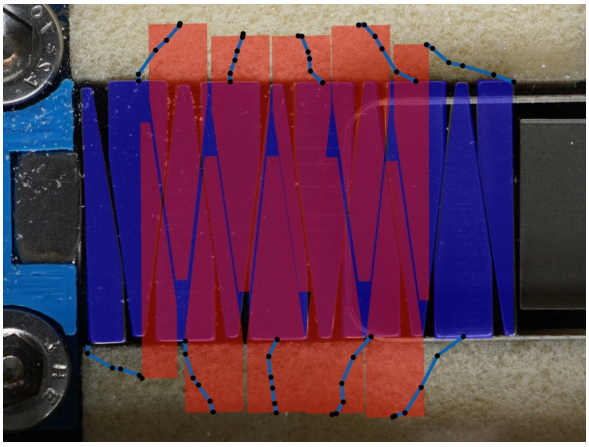

Figure 6.1: *Example wedge path visualization. The wedges in collapsed state (blue) expand along the expansion path (blue line with black dots) to the maximum expansion state (red).*

6.2. Experiment 2: In-pedicle expansion and lateral loading

Figure 6.4 shows images of the three experiments including the outline of the wedges before the experiment (red) and after the experiment (blue). The central bolt of both situations are aligned, to show whether the wedges have shifted with respect to the central bolt. The black dots indicate the contact points with the pedicle cortex before the experiment. The contact length measurement indicates the distance between the two outermost contact points. Table 6.1 shows an overview of the number of contact points and the contact length after the expansion of the prototype and before the experiment.

In Figure 6.5 the resulting displacement angle of the prototype and mock-up model is plotted against the lateral input force (caudal in Figure 6.5a and cranial in Figure 6.5b).

7. Discussion

7.1. Main findings

The expandable in-pedicle anchor proposed in this thesis is designed to overcome the problem of toggling that can occur in current anchoring solutions for spinal fusion surgery. A proof-of-principle prototype has been developed based on the ability of a wedge to change the direction of a force laterally. The manufactured proof-of-principle prototype uses ten wedges with a central bolt with flattened sides as a core. The prototype can be easily applied in two steps by inserting the prototype into a pre-drilled hole and applying a compressive force by tightening a nut on this bolt. This results in a lateral expansion of the wedges and thereby a change in the macro-shape of the prototype. It was experimentally shown that the wedges were able to successfully expand within 5 and 10 PCF Sawbones solid foam, which have similar properties to osteoporotic cancellous bone. The wedges show a general tendency to move towards the middle due to the shortening of the prototype. Consequently, the bolt moves slightly out of the pedicle posteriorly during expansion, which is an important observation for further development of the in-pedicle anchor.

Moreover, the distribution of the contact points with the pedicle cortex is improved. In a pedicle screw, the contact with the pedicle cortex is limited to two flanks of the screw and there is no contact with the top and bottom of the pedicle. This prototype has contact with the top and bottom of the pedicle, thereby possibly increasing the stability. A conventional pedicle screw only contacts the cortical pedicle with a limited number of threads. In an ideal scenario, this would result in a contact length of approximately 4-6 mm along the sides of the pedicle screw (two or three threads of 2 mm pitch) with 4 or 5 contact points. However, in practice often a smaller screw diameter is chosen to reduce the risk of neurological damage, which drastically reduces the contact length and number of contact points or often leads to no pedicle contact at all [26]. The presented prototype reached an average contact length of 6.35mm (real scale) with the top and bottom of the pedicle with an average of six contact points. In theory for this prototype, the contact length could be improved to 11.2 mm with a maximum of nine contact points.

Under lateral forces, the prototype rotates less in the designed pedicle model than an unexpanded solid mock-up prototype with the same dimensions, both in caudal and in cranial direction. The average angular displacement at maximum load was 7.0x smaller in the cranial direction and 4.5x smaller in the caudal direction for the proof-of-principle prototype compared to the mock-up model. This does not necessarily demonstrate that the prototype has better toggling properties than a conventional pedicle screw, but does indicate that the addition of the proposed shape-adaptive mechanism to an in-pedicle anchor can improve its resistance to rotating under lateral load. To demonstrate whether the proposed mechanism has clinical added value due to better toggling properties than a pedicle screw. Several aspects of the designed prototype still need further investigation and improvement.

7.2. Limitations and Future Research

7.2.1. Design

Although the prototype seemed to fixate relatively well in the pedicle model during the first and third attempts, during the second trial the wedges slid with respect to the central bolt. This should not be possible; the proto-

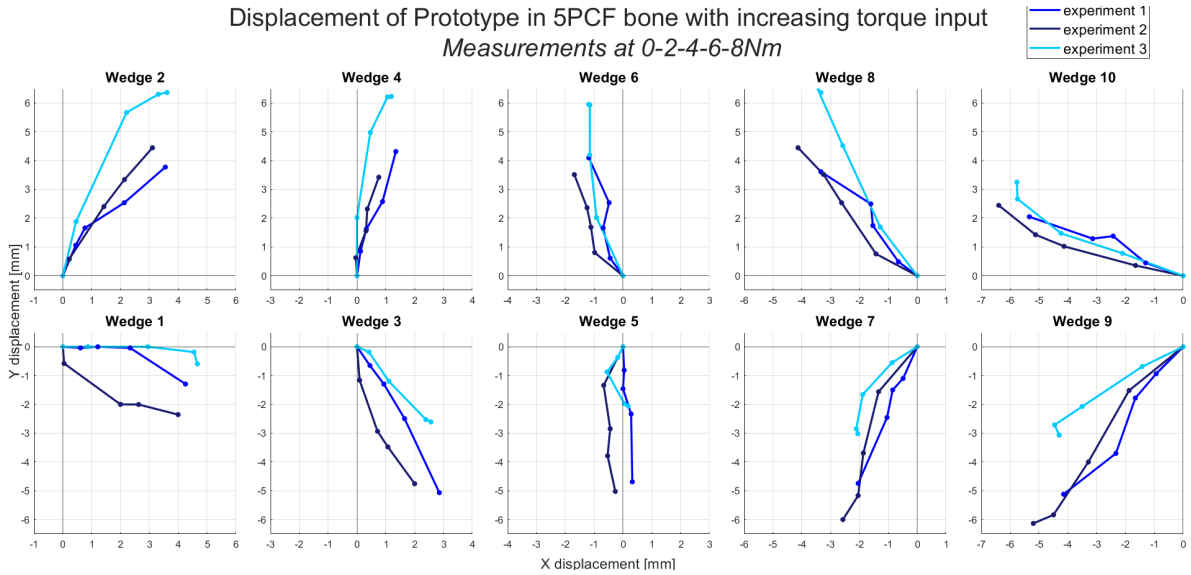

Figure 6.2: *The expansion paths results of Experiment 1: Cancellous Bone Compression showing three different 50 PCF repetitions. Measurements at 0-2-4-6-8Nm*

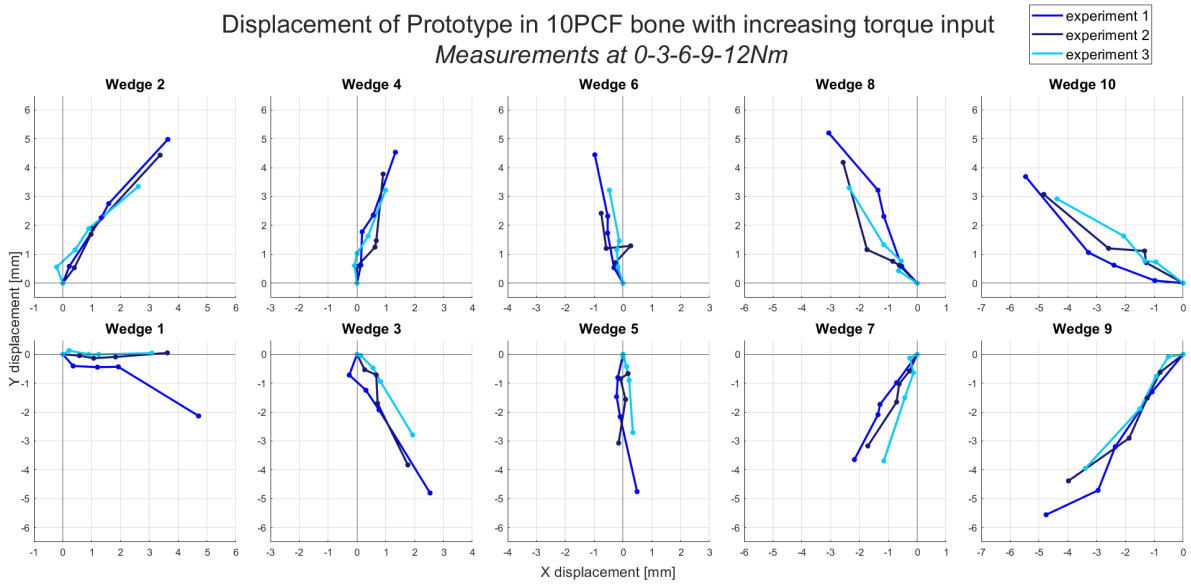

Figure 6.3: *The expansion paths results of Experiment 1: Cancellous Bone Compression showing three different 10 PCF repetitions. Measurements at 0-3-6-9-12Nm*

Table 6.1: *Contact points and contact length after expansion in Experiment 2: In-pedicle expansion and lateral loading*

	Exp 1	**Exp 2**	**Exp 3**	**AVG**	**STD**
Contact Points	7	7	6	6.7	0.6
Contact Length [mm]	13.5	13.7	11.0	12.7	1.5

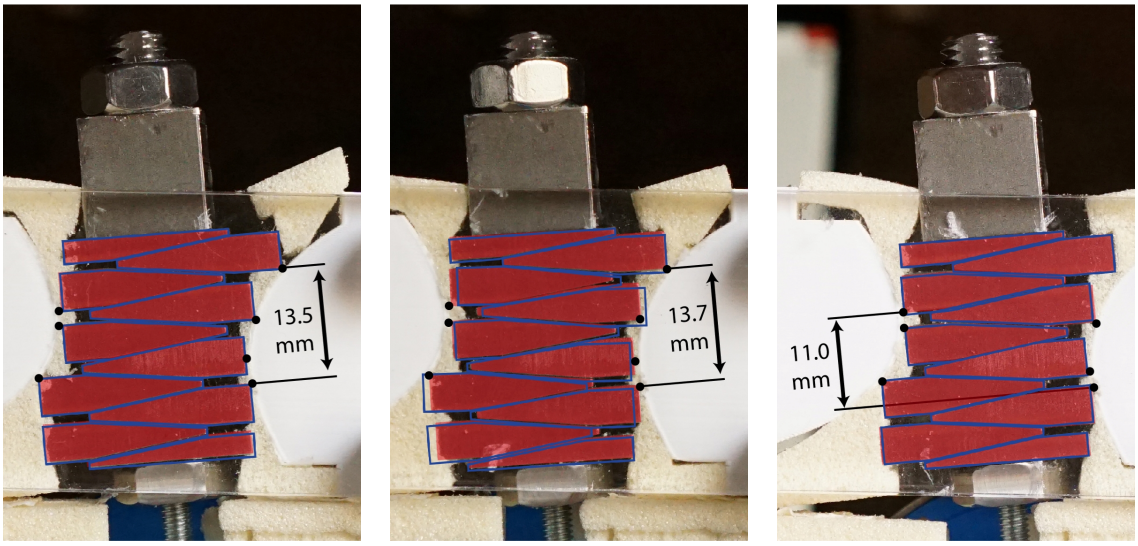

(a) *Photo after the first experiment* ***(b)*** *Photo after the second experiment* ***(c)*** *Photo after the third experiment*

Figure 6.4: *Images of the proof-of-principle prototype before Experiment 2: In-pedicle expansion and lateral loading (red wedges) and at the maximum caudal load (blue outline). The central bolts are aligned. The black dots show the contact points of the anchor with the pedicle cortex before the experiment. The contact length (200% scale) is determined by measuring the distance between the two most outer contact points.*

type should act as a solid object. In both experiments the first and last wedge both mostly moved horizontally and did not expand vertically as much as the other wedges. A possible explanation for this is that the friction force is directed vertically between the first wedge and the head of the bolt and between the last wedge and the nut. This makes the expansion more difficult for these two wedges than for the middle wedges in this prototype.

2D to 3D

The current 2D prototype, pedicle model, and experiments also do not do full justice to the in-body conditions that will take place in a clinical setting. First of all, a way to make this mechanism 3D has to be considered. To get from our 2D proof-of-principle prototype to a functional 3D concept with the same working principle there are two basic approaches: use the wedge expansion as the only fixation mechanism (Figure 7.1a) or combine the wedge expansion mechanism for the caudocranial fixation with a different lateral fixation, such as a conventional pedicle screw (Figure 7.1b). These two concepts are worked out into two example 3D models. The first 3D concept uses a central bolt that is flattened from two angles to fit in the diagonal guiding tracks of the wedges. The wedges have slanted sides that on one side are oriented horizontally and at the other end vertically. By using a nut to add a compressive force to the wedges, the wedges expand along the designated diagonal tracks. The other concept uses a conventional pedicle screw with a central cavity for a bolt and a square recess to allow placement of multiple wedges and a nut in the middle. The wedges are threaded to facilitate an easy rotational insertion in the pedicle. When the bolt is turned the wedges contract due to the compressive force of the nut. There are multiple other options for a 3D wedge-based in-pedicle anchor, but these two options give insight into how a possible clinical product could look.

Scalability

A new 3D prototype downsized to real scale could give insight into the scaling of the different forces involved in the expansion of the prototype. The forces needed to expand are smaller due to the decreased contact surface with the cancellous bone, but the maximum input force that can be delivered could also be lower due to the use of a smaller central bolt. In addition, it will be necessary to investigate whether the real-scale prototype and in particular the central bolt can withstand the in-pedicle forces. The maximum expansion will probably scale down a bit more than 200%, because the parts can be scaled down twice, but the size of some part features cannot be scaled by that amount anymore to keep sufficient strength.

Clinical implementation

The stainless steel (316L) used in the prototype is less corrosion resistant than other materials more regularly used for long-term implants such as titanium- or cobalt-based alloys. The use of stainless steel can lead to toxicity and allergic reactions to debris caused by device degradation [33]. Changing the material to a more corrosion-resistant material also changes the frictional

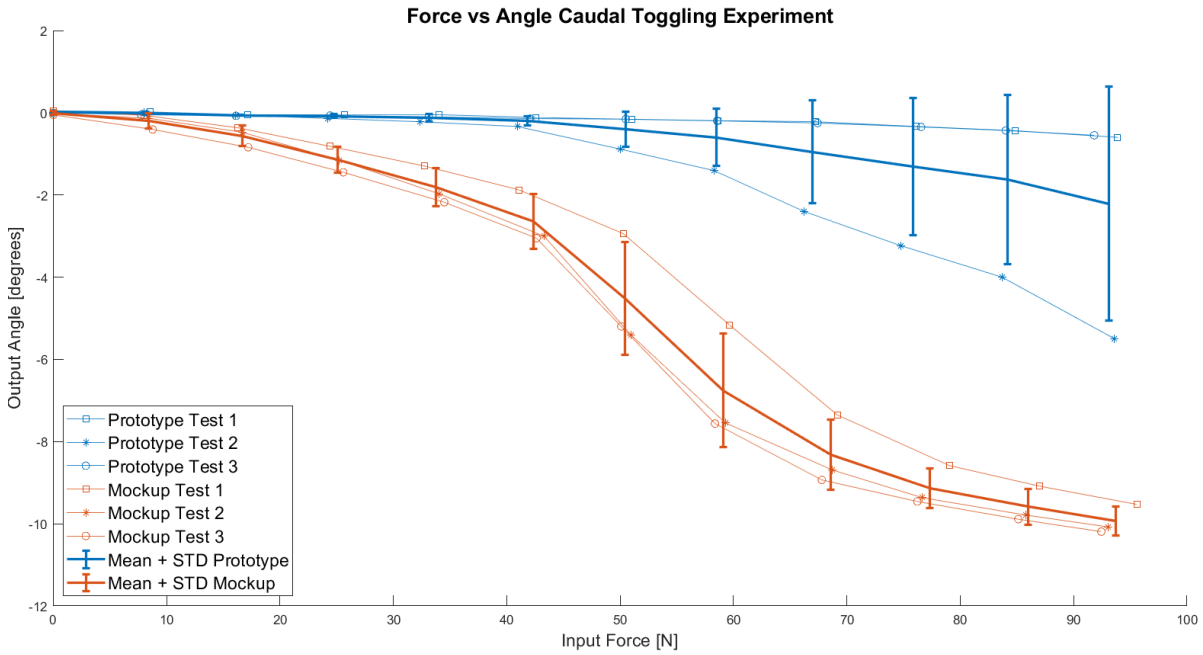

(a) *Caudal Graph*

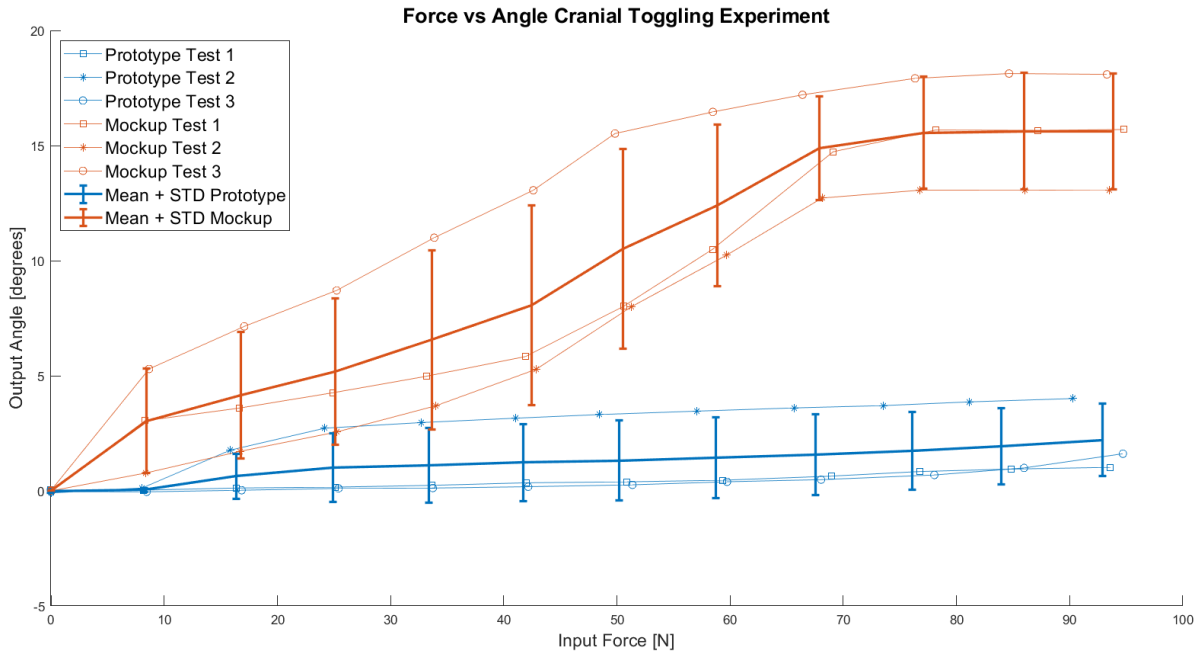

(b) *Cranial Graph*

Figure 6.5: *Results of Experiment 2: In-pedicle expansion and lateral loading*

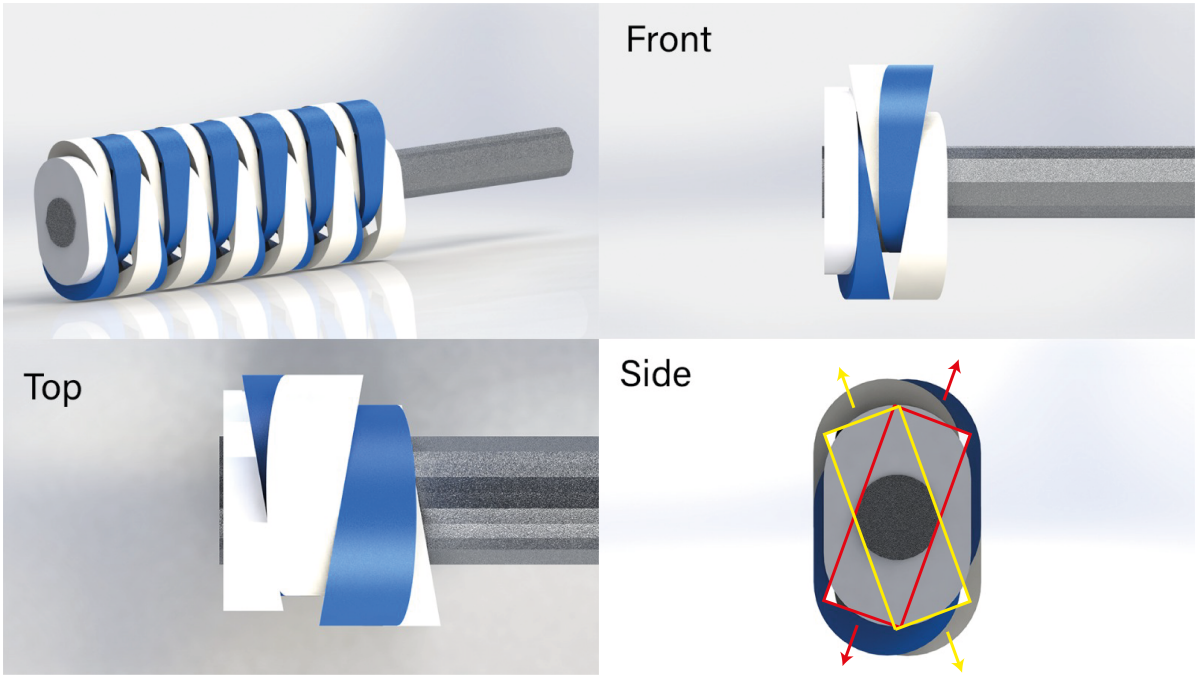

(a) *A new concept using wedges that can expand both horizontally and vertically by using wedges with diagonal guiding tracks. In yellow and red, respectively, the tracks and expansion directions of the white and blue wedges are indicated.*

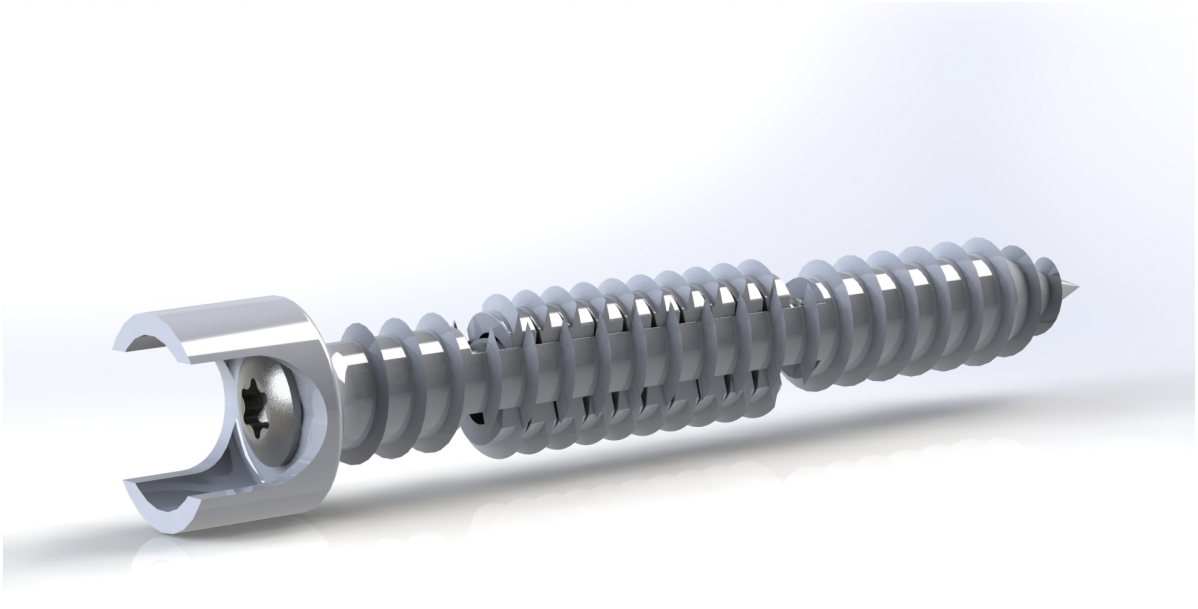

(b) *An adaptation of a conventional pedicle screw to include expandable wedges.*

Figure 7.1: *Two possible future in-pedicle anchors using the wedge working principle.*

properties of the wedges. Whether this has consequences for the functioning of the prototype needs to be investigated. Possible problems can be alleviated by changing the inclination angle or adding a low-friction coating such as Diamond-Like Carbon (DLC) [34].

Due to the choice for a friction-based system there can be a force buildup in some of the wedges while others may not have fully expanded yet. Moreover, the system is designed in the ideal scenario to fill the pedicle fully and be rigid. These two factor can cause local stress on the pedicle cortex, especially at the corners of the currently used flat compression surfaces of the wedges. This can cause fractures of the pedicle or vertebra due to the expansion forces during placement or due to external forces caused by daily activities of the patient. The ideal in-pedicle anchor, therefore, has more rounded wedges to prevent high local stresses and some flexibility between the anchor and the pedicle cortex to prevent high local stress and resulting dangerous complications. Possible solutions for this are, for example, the use of a more flexible material, the addition of padding on the contact surface or an engineered point of failure of the implant when stresses on the pedicle become too high.

Another aspect that should be considered in further development is the fact that bone is a living substance. This means that, according to Wolff's law, local stresses caused by or removed by a metal implant can lead to a local increase or reduction in Bone Mineral Density (BMD), respectively. Both the short and long term influence of the implant on the local bone growth should be investigated, including the osseointegration of the implant and its influence on the stability and removability of the implant. Finally, several aspects deserve extra attention when developing this prototype further into a clinically usable product, such as the alignment of the implant during expansion and the need for a tool that can help a surgeon apply the required torques.

Although there are still a lot of factors that should be investigated before the proposed expansion mechanism can be deployed in a clinical application the results show improved resistance to lateral rotation and an increased number of contact points with the pedicle cortex along the length of an in-pedicle anchor. This provides a hopeful picture for a possible future clinical application.

7.2.2. Validation Experiments

The data from Experiment 1: Bone Compression Experiment shows that there is a large standard deviation for almost all measurements. Firstly, this is because the measurement method of determining dimensions from pictures has limited accuracy. However, the biggest factor seems to be that the wedge expansion paths are not exactly repeatable. There are a lot of factors that influence the exact path of each of the wedges at each moment. Examples of these influences are small deviations in the way the torque is applied to the nut, deviations in the local density of the bone foam, and small deviations in the start position between the different measurements. Besides this, the torque wrench does not only apply torque but also an in-plane vertically directed force to the nut-end of the prototype. To minimize the influence of all these variables, the prototype could have been supported from two sides to keep the central axis straight and the application of the torque the same every time.

The torque applied to the nut also tended to rotate the extension tube due to friction. This resulted in more contact between the extension tube and the PMMA. The resulting frictional component between these two surfaces could have been different for each sub-experiment resulting in a less accurate measurement.

The same inaccuracy due to friction between the extension tube and the PMMA can be observed in Experiment 2: Toggling Experiment. Furthermore, it can be seen in displacement angle graphs that a steady-state is not reached every time before a new weight was added to the hook. This limits the accuracy of the exact data points, but the generic comparison between the prototype and the mock-up model still holds. The cranial measurement that has been made cannot be seen as a stand-alone measurement, because it is preceded by a caudal load experiment. The displacement by the caudal force may therefore have influenced the measurement of the displacement by the cranial force.

For future research it would be interesting to perform a combined cyclic load test with an axial pull-out test of a 3D prototype can provide a better insight into whether the prototype can compete with the current golden standard of a pedicle screw in toggling behavior and pull-out resistance, as well as in resistance to bending or breaking. It would be especially interesting to perform these future experiments in real bone. The used densities of Sawbones Rigid Foam have similar mechanical properties as human osteoporotic bone, but its properties are much more homogeneous. Local higher densities of real cancellous bone could influence the ability of the prototype to expand. It would also be interesting to test whether higher densities of cancellous bone can be compressed by using a different material or inclination angle to reduce friction or by using spikes or cutting edges on the outer surface of the wedges. An additional advantage of these in-body experiments is that it can be tested whether the prototype can adapt to the different patient-specific pedicle anatomy and bone properties.

8. Conclusion

In this thesis, an expandable in-pedicle anchor is proposed to increase the resistance to toggling of a spinal fusion pedicle anchor. The in-pedicle anchor can be inserted into a pre-drilled cavity through the pedicle and expanded by tightening a nut on the bolt. A 2D scaled-up proof-of-principle prototype has been made, consisting of ten wedges and a central bolt with flattened sides. During experiments, the in-pedicle anchor has shown to be able to compress osteoporotic solid bone foam of both 5 and 10 PCF. The proof-of-principle prototype is able to adapt its shape to the internal shape of the pedicle cortex and made contact possible with the top and bottom of the pedicle cortex, in contrast with contact of a conventional pedicle screw at only the two flanks. The proof-of-principle prototype had an average of six contact points during testing with a contact length between the two outer most points of 6.35mm (scaled to 100%). The expanded proof-of-principle prototype had an average angular displacement of 2.2° in both caudal and cranial direction at a lateral load of circa 100 N. For a rigid mockup model with the same dimensions as the unexpanded proof-of-principle prototype, these displacements were, respectively, 4.5x and 7x larger. In future research, it would be interesting to see an in-bone experiment using a real-scale 3D prototype. In particular, the rigidity of the prototype and local stresses that can occur and the effect this has on the integrity of the pedicle should be considered. The presented proof-of-principle prototype demonstrates the operation of the wedge expansion principle and shows promising first results for a future clinical application of a wedge expansion mechanism to improve the toggling resistance of spinal fusion bone anchors.

References

[1] *Most Common Operations in Hospital Inpatient Stays - HCUP Fast Stats*. URL: https://www.hcup-us.ahrq.gov/faststats/NationalProceduresServlet?year1=2018&characteristic1=0&included1=1&year2=2010&characteristic2=31&included2=1&expansionInfoState=hide&dataTablesState=hide&definitionsState=hide&exportState=hide (visited on 11/30/2021).

[2] *Costs for Spine Fusions*. URL: https://www.ahrq.gov/data/infographics/spine-fusions.html (visited on 11/30/2021).

[3] Shehryar Rahim Sheikh et al. "Can we justify it? Trends in the utilization of spinal fusions and associated reimbursement." In: *Neurosurgery* 86.2 (2020), E193–E202.

[4] Sean S Rajaee et al. "Spinal fusion in the United States: analysis of trends from 1998 to 2008." In: *Spine* 37.1 (2012), pp. 67–76.

[5] Christopher D Chaput et al. "Reduction in radiation (fluoroscopy) while maintaining safe placement of pedicle screws during lumbar spine fusion." In: *Spine* 37.21 (2012), E1305–E1309.

[6] *Spinal fusion*. URL: https://www.mayoclinic.org/tests-procedures/spinal-fusion/about/pac-20384523 (visited on 04/05/2022).

[7] Ziquan Li et al. "Cement leakage following percutaneous kyphoplasty in a patient after a posterior lumbar fusion: a case report." In: *BMC surgery* 20.1 (2020), pp. 1–6.

[8] Se-Il Suk et al. "Thoracic Pedicle Screw Fixation in Spinal Deformities: Are They Really Safe?" In: *Spine* 26.18 (Sept. 15, 2001), pp. 2049–2057. ISSN: 0362-2436. URL: https://journals.lww.com/spinejournal/Abstract/2001/09150/Thoracic_Pedicle_Screw_Fixation_in_Spinal.22.aspx (visited on 01/18/2022).

[9] Mario Di Silvestre et al. "Complications of Thoracic Pedicle Screws in Scoliosis Treatment." In: *Spine* 32.15 (July 1, 2007), pp. 1655–1661. ISSN: 0362-2436. DOI: 10.1097/BRS.0b013e318074d604. URL: https://journals.lww.com/spinejournal/Abstract/2007/07010/Complications_of_Thoracic_Pedicle_Screws_in.14.aspx (visited on 01/18/2022).

[10] Timothy R. Kuklo and Ronald A. Lehman. "Effect of various tapping diameters on insertion of thoracic pedicle screws: a biomechanical analysis." In: *Spine* 28.18 (Sept. 15, 2003), pp. 2066–2071. ISSN: 1528-1159. DOI: 10.1097/01.BRS.0000084665.31967.02.

[11] Toru Hirano et al. "Structural Characteristics of the Pedicle and Its Role in Screw Stability." In: *Spine* 22.21 (Nov. 1, 1997), pp. 2504–2510. ISSN: 0362-2436. URL: http://journals.lww.com/spinejournal/Fulltext/1997/11010/Structural_Characteristics_of_the_Pedicle_and_Its.7.aspx (visited on 11/30/2021).

[12] Zi-xiang Wu et al. "A comparative study on screw loosening in osteoporotic lumbar spine fusion between expandable and conventional pedicle screws." In: *Archives of Orthopaedic and Trauma Surgery* 132.4 (Apr. 1, 2012), pp. 471–476. ISSN: 1434-3916. DOI: 10.1007/s00402-011-1439-6. URL: https://doi.org/10.1007/s00402-011-1439-6 (visited on 11/30/2021).

[13] B. G. Santoni et al. “Cortical bone trajectory for lumbar pedicle screws.” In: *The Spine Journal* 9.5 (May 1, 2009), pp. 366–373. ISSN: 1529-9430. DOI: 10.1016/j.spinee.2008.07.008. URL: https://www.sciencedirect.com/science/article/pii/S1529943008007213 (visited on 11/30/2021).

[14] Elaine Marieb and Katja Hoehn. *Human Anatomy & Physiology, Global Edition*. 10th edition. Pearson, 2015. ISBN: 978-1-292-09697-1.

[15] M. M. Panjabi et al. “Complexity of the thoracic spine pedicle anatomy.” In: *European Spine Journal* 6.1 (Jan. 1997), pp. 19–24. ISSN: 0940-6719. DOI: 10.1007/BF01676570. URL: https://www.ncbi.nlm.nih.gov/pmc/articles/PMC3454633/ (visited on 11/30/2021).

[16] H. Defino and J. Vendrame. “Role of cortical and cancellous bone of the vertebral pedicle in implant fixation.” In: *European Spine Journal* 10.4 (Aug. 2001), pp. 325–333. ISSN: 0940-6719. DOI: 10.1007/s005860000232. URL: https://www.ncbi.nlm.nih.gov/pmc/articles/PMC3611516/ (visited on 11/30/2021).

[17] *NCI Dictionary - Spine*. URL: https://www.cancer.gov/publications/dictionaries/cancer-terms/def/spine (visited on 04/05/2022).

[18] Fras Dakhil-Jerew et al. “Inter-observer reliability of detecting Dynesys pedicle screw using plain X-rays: a study on 50 post-operative patients.” In: *European Spine Journal* 18.10 (Oct. 2009), pp. 1486–1493. ISSN: 0940-6719. DOI: 10.1007/s00586-009-1071-0. URL: https://www.ncbi.nlm.nih.gov/pmc/articles/PMC2899385/ (visited on 11/30/2021).

[19] Dieter Grob et al. “Clinical Experience With the Dynesys Semirigid Fixation System for the Lumbar Spine: Surgical and Patient-Oriented Outcome in 50 Cases After an Average of 2 Years.” In: *Spine* 30.3 (Feb. 1, 2005), pp. 324–331. ISSN: 0362-2436. DOI: 10.1097/01.brs.0000152584.46266.25. URL: http://journals.lww.com/spinejournal/Fulltext/2005/02010/Clinical_Experience_With_the_Dynesys_Semirigid.12.aspx (visited on 11/30/2021).

[20] Klaus John Schnake, Stefan Schaeren, and Bernard Jeanneret. “Dynamic Stabilization in Addition to Decompression for Lumbar Spinal Stenosis with Degenerative Spondylolisthesis.” In: *Spine* 31.4 (Feb. 15, 2006), pp. 442–449. ISSN: 0362-2436. DOI: 10.1097/01.brs.0000200092.49001.6e. URL: http://journals.lww.com/spinejournal/Fulltext/2006/02150/Patient_Outcomes_After_Decompression_and.12.aspx?casa_token=6Wfg-bJFyTMAAAAA:1_GW59nBTEQy_Tdh3aG7962YTUnLYj_nua1B7Lms6Qu0mr94WJcTbF3hIKmGyfpMBFPj6jwlXFerhWsxV6cgfQO77A0 (visited on 11/30/2021).

[21] B. Sandén et al. “The significance of radiolucent zones surrounding pedicle screws.” In: *The Journal of Bone and Joint Surgery. British volume* 86-B.3 (Apr. 1, 2004). Publisher: The British Editorial Society of Bone & Joint Surgery, pp. 457–461. ISSN: 0301-620X. DOI: 10.1302/0301-620X.86B3.14323. URL: https://online.boneandjoint.org.uk/doi/abs/10.1302/0301-620x.86b3.14323 (visited on 11/30/2021).

[22] Dirk W. Kiner et al. “Biomechanical Analysis of Different Techniques in Revision Spinal Instrumentation: Larger Diameter Screws: Versus: Cement Augmentation.” In: *Spine* 33.24 (Nov. 15, 2008), pp. 2618–2622. ISSN: 0362-2436. DOI: 10.1097/BRS.0b013e3181882cac. URL: http://journals.lww.com/spinejournal/FullText/2008/11150/Biomechanical_Analysis_of_Different_Techniques_in.8.aspx?casa_token=nsMN2zQLPYIAAAAA:AGkGRW4LF-7-_MSUnUWgnPCR5x2mQse7_dUxkS0ALGGB4u6eSSkSQUr8ELzqTcsdADXapmEWONfJeTnoNETAgtILyFE (visited on 11/30/2021).

[23] Theodore J. Choma et al. “Biomechanical Analysis of Pedicle Screws in Osteoporotic Bone With Bioactive Cement Augmentation Using Simulated In Vivo Multicomponent Loading.” In: *Spine* 36.6 (Mar. 15, 2011), pp. 454–462. ISSN: 0362-2436. DOI: 10.1097/BRS.0b013e3181d449ec. URL: http://journals.lww.com/spinejournal/fulltext/2011/03150/biomechanical_analysis_of_pedicle_screws_in.8.aspx?casa_token=P1y1mvJN-_YAAAAA:shgTT_UAsHyLkMkzmc8DkGmq7PpUFNgm-rY_ZvySCM21Nq8Zn8tqiELU11Cjw0nK-KZsYiQSsgPD-jEM3F28B6IyH4k (visited on 11/30/2021).

[24] Chad Waits, Douglas Burton, and Terence McIff. “Cement Augmentation of Pedicle Screw Fixation Using Novel Cannulated Cement Insertion Device.” In: *Spine* 34.14 (June 15, 2009), E478. ISSN: 0362-2436. DOI: 10.1097/BRS.0b013e3181a8f663. URL: http://journals.lww.com/spinejournal/fulltext/2009/06150/Cement_Augmentation_of_Pedicle_Screw_Fixation.19.aspx?casa_token=AYycml3l__0AAAAA:4mjfvZs7MQWznyIaNvshqPntZjGUud8mjXO

pQqqPBOBO3HCBJ2Eb8ip4BMOOri3AT5xh _ ifMQE9x9OBh7c2MeD _ NeYY (visited on 11/30/2021).

[25] Rebecca Anne Murray. "Pedicle screw fixation." Accepted: 2014-09-17T13:16:54Z ISBN: 9781312520196 Journal Abbreviation: Pedikelschrauben Fixierung. Thesis. Technische Universität Hamburg, 2014. DOI: 10.15480/882.1186. URL: https://tore.tuhh.de/handle/11420/1188 (visited on 11/30/2021).

[26] E. P. H. A. Verdult. "Design of a directional drilling device and development of a new spinal anchoring technique." In: (1998). URL: https://repository.tudelft.nl/islandora/object/uuid%3A31d0606c-8f66-422d-a24c-f73b2a4cebe4 (visited on 11/30/2021).

[27] A. Rohlmann, G. Bergmann, and F. Graichen. "Loads on an internal spinal fixation device during walking." In: *Journal of Biomechanics* 30.1 (Jan. 1997), pp. 41–47. ISSN: 0021-9290. DOI: 10.1016/s0021-9290(96)00103-0.

[28] A Devaraju. "A review on important factors affecting dry sliding friction." In: *Journal of Surface Science and Technology* 32.3-4 (2016), pp. 73–78.

[29] *Frictional properties of stainless steels – British Stainless Steel Association*. URL: https://bssa.org.uk/bssa_articles/frictional-properties-of-stainless-steels/ (visited on 02/04/2022).

[30] *Top Biomechanical Products & Materials Provider for Testing & Validation*. URL: https://www.sawbones.com/biomechanical-product-info (visited on 11/30/2021).

[31] Lis Mosekilde. "Vertebral structure and strengthIn vivo andIn vitro." In: *Calcified tissue international* 53.1 (1993), S121–S126.

[32] Otávio Teixeira Pinto et al. "A New Test Method for In Vitro Evaluation of Pedicle Screw Loosening Potential." In: *Journal of Medical Devices* 15.4 (Oct. 18, 2021). ISSN: 1932-6181. DOI: 10.1115/1.4052517. URL: https://doi.org/10.1115/1.4052517 (visited on 01/20/2022).

[33] Zhong Li and Khiam Aik Khor. "Preparation and Properties of Coatings and Thin Films on Metal Implants." In: *Encyclopedia of Biomedical Engineering*. Ed. by Roger Narayan. Oxford: Elsevier, 2019, pp. 203–212. ISBN: 978-0-12-805144-3. DOI: https://doi.org/10.1016/B978-0-12-801238-3.11025-6. URL: https://www.sciencedirect.com/science/article/pii/B9780128012383110256.

[34] Geoffrey Dearnaley and James H Arps. "Biomedical applications of diamond-like carbon (DLC) coatings: A review." In: *Surface and Coatings Technology* 200.7 (2005), pp. 2518–2524.

[35] Bing Li et al. "Accurate Determination of Isthmus of Lumbar Pedicle: A Morphometric Study using Reformatted Computed Tomographic Images." In: *Spine* 29.21 (Nov. 1, 2004), pp. 2438–2444. ISSN: 0362-2436. DOI: 10.1097/01.brs.0000144355.50660.65. URL: http://journals.lww.com/spinejournal/fulltext/2004/11010/Accurate_Determination_of_Isthmus_of_Lumbar.17.aspx?casa_token=6XI9KLr55PoAAAAA:iIr73NMO1a6Oy5Ni40r4oYq3Bia9ckCqEm0mo7stZmQm49y90MXmu0lWageHTIBGN1PNrdY_9PsggYAp9sDijvhNwec (visited on 11/30/2021).

[36] Shankar Acharya, Tsewang Dorje, and Abhishek Srivastava. "Lower Dorsal and Lumbar Pedicle Morphometry in Indian Population: A Study of Four Hundred Fifty Vertebrae." In: *Spine* 35.10 (May 1, 2010), E378. ISSN: 0362-2436. DOI: 10.1097/BRS.0b013e3181cb7f2b. URL: https://journals.lww.com/spinejournal/Fulltext/2010/05010/Lower_Dorsal_and_Lumber_Pedicle_Morphometry_in.16.aspx?casa_token=sQyujA-ZpcgAAAAA:tcnsILT0zY7YwL61u_jdS-jmdgPx2K96lVmJDCfpDcmOt_90kshlgknJJIpELDnjs7wjyBqtWk-BvHhBusHZwqUboQQ (visited on 02/01/2022).

[37] Michaela Gstoettner et al. "Inter- and intraobserver reliability assessment of computed tomographic 3D measurement of pedicles in scoliosis and size matching with pedicle screws." In: *European Spine Journal* 20.10 (July 19, 2011), p. 1771. ISSN: 1432-0932. DOI: 10.1007/s00586-011-1908-1. URL: https://doi.org/10.1007/s00586-011-1908-1 (visited on 11/30/2021).

[38] B. Sevastik et al. "Vertebral rotation and pedicle length asymmetry in the normal adult spine." In: *European Spine Journal* 4.2 (Apr. 1, 1995), pp. 95–97. ISSN: 1432-0932. DOI: 10.1007/BF00278919. URL: https://doi.org/10.1007/BF00278919 (visited on 11/30/2021).

[39] *Screw thread mechanics*. URL: http://www-mdp.eng.cam.ac.uk/web/library/enginfo/textbooks_dvd_only/DAN/threads/mechanics/mechanics.html (visited on 04/05/2022).

Appendix A: Design of Simplified Pedicle Model

A.1. Simplified Pedicle Model

The complex internal shape of the pedicle cannot be translated to a model easily. Therefore, the choice was made to reduce the internal cross-sectional shape to an oval tunnel with a certain width and height at both the isthmus (f) and both ends of the pedicle (i and k). The cortex is reduced to a rectangular block to ease fabrication of an eventual physical model. To make an accurate model of the internal pedicle dimensions of the internal pedicle are needed. Morphometry studies on pedicles in the lower back are scares. Especially studies that include all needed dimensions and are performed on a general population.

Because of this, and because most papers [35, 36] only measure the internal cross section at the isthmus, the cross sections at both ends of the pedicle had to be deducted in some other way.

A CT scan of a lumbar pedicle out of the paper of Li *et al.* was used as the basis for the geometry of the pedicle model. The average measured data of the internal or endosteal width and height of the pedicle of 41 patients of Chinese decent was combined with the geometry of a pedicle of one single CT scan to create a model [35].

A.2. Deduction of internal dimensions

This was done by taking the average internal width at the isthmus for the transversal cross section and determining all other dimensions based on this average data (see Figure A.1a). The same is done using the internal height for the sagittal cross section (see Figure A.1b). The results of the study of Li *et al.* [35] were split in measurements on male and female subject.The mean of the male measurements were taken as the basis for our model because of the slightly larger dimensions. The width/height ratios and cortical thicknesses are almost the same for both sexes, so the concept can be scaled down for application in the smaller female pedicles.

A.3. Deduction of the pedicle length

The definition of the pedicle length is a bit arbitrary and therefore defined in different ways in multiple papers. Some papers use the length from the dorsal edge of the vertebral body to the articular process [37]. Other use the length from the dorsal edge of the vertebral body to the mid-axis of the transverse processor [38], or even to the posterior longitudinal ligament [35]. Because we are only interested in the length of the pedicle that contains the biggest part of the curvature of the pedicle we chose to use the definition of Sevastik *et al.* [38] with a small change.

First the longitudinal axis of the vertebra (a) and the orthogonal tangent of the dorsal edge of the vertebral body (b) are drawn. Next the mid-axis of the transverse process is deducted by drawing a line from the intersection of a and b to the middle of the end of the transverse process (line d). The pedicle length is then defined as the distance between lines d and b along the midline of the pedicle (c). Unfortunately Sevastik *et al.* [38] does not mention any quantitative measurements so our values cannot be compared. All deducted dimensions can be seen in Table A.2.

A.4. Transition between cancellous and cortical bone

The dimensions that are presented in the paper (Table A.1), are the inner and outer dimensions of the cortical shell. This shell is filled with cancellous bone that should be (partially) removed before placing the anchor. The boundary between the cortical and cancellous in the different pedicles is described as “smooth and clear in L1 but gradually became abnormal below it”. Therefore, we assume for our L1 pedicle model that this boundary is clear and that there is no transition zone between the two bone types to simplify the model.

As shown in Table A.1, the pedicle cortex is not equally thick around the pedicle. The central cavity and internal cancellous bone are thus not perfectly centered. For our model this is not important, because the focus lays on the internal shape of the pedicle.

A.5. Central tunnel

During surgery common practice is to tap with a diameter that is 1mm smaller than the screw diameter [3]. There is not a lot of data on what screw diameter is mostly used in each pedicle. However, one rule of thumb that is sometimes used is that the screw diameter should be 80% of the pedicle width [8, 9]. In case of the L1 pedicle this would result in the usage of either a 6 or 6.5mm screw. Because of this we assume that, in a clinal application, a tunnel can be created by drilling two half-overlapping holes using a 5.5mm drill or tap. This tunnel will mostly remove cancellous bone and a small amount of cortical bone around the isthmus. The tunnel is centered and follows the horizontal center line of pedicle. The resulting simplified pedicle model can be seen in Figure A.2.

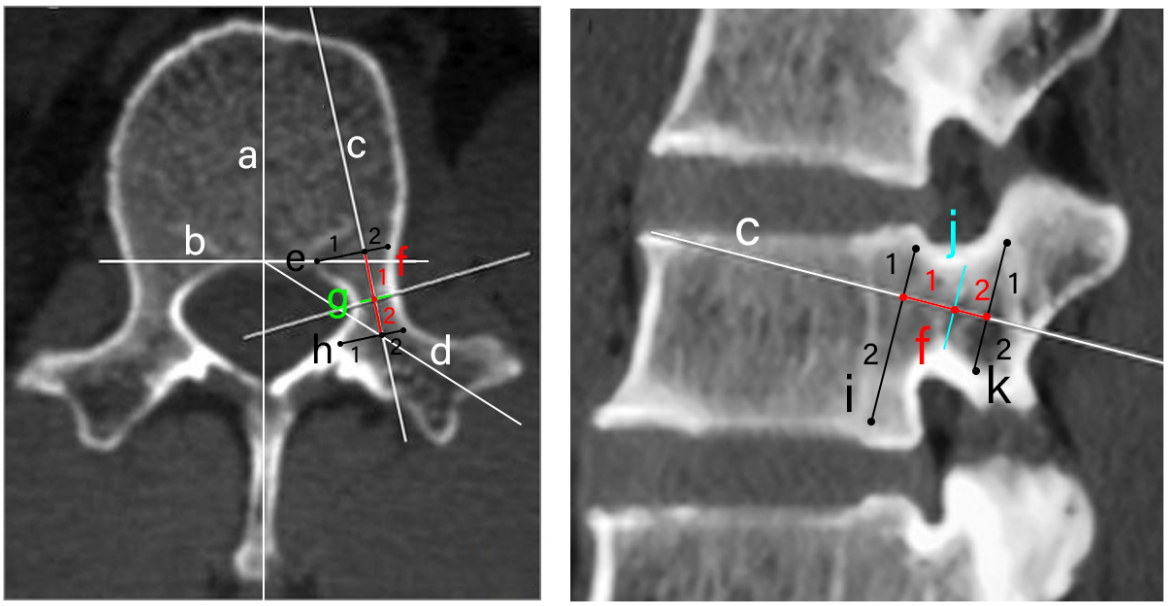

Figure A.1: *CT scans from the paper of Li et al. [35]. a) Transverse scans showing the deducted dimensions b) Sagittal scans showing the deducted dimensions*

Isthmus	Male dimensions
Outer Width	7.9 mm
Inner width (g)	5.2 mm
Outer Height	18.3 mm
Inner Height (j)	11.1 mm
Cortical Thickness	
Superior	3.2 mm
Inferior	3.6 mm
Medial	1.5 mm
Lateral	2 mm

Table A.1: *Average measured data of the pedicle[35]*

Sagittal Plane	Male Dimension
e1	4.2 mm
e2	8.3 mm
f1	8.3 mm
f2	6.3 mm
h1	7.5mm
h2	3.7 mm
Transversal Plane	
i1	7.6 mm
i2	17.3 mm
k1	10.9 mm
k2	8.5 mm

Table A.2: *Deducted dimensions for the simplified pedicle model*

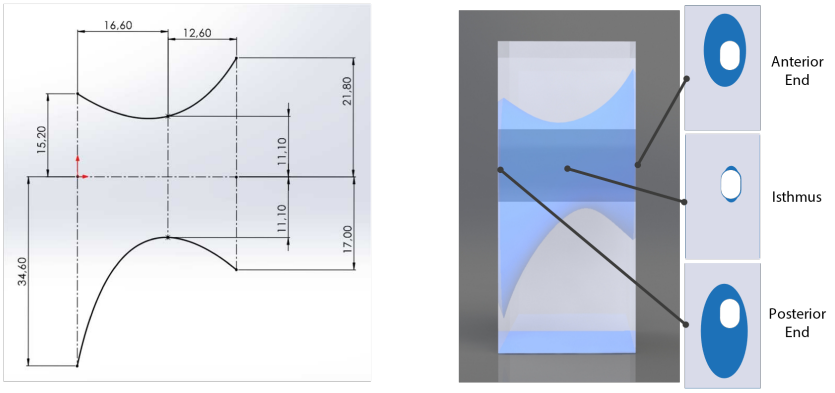

Figure 17 The pedicle model. a) The two polylines that describe the 2D shape of the pedicle. b) The 3D model of the pedicle including cross sections at the isthmus and both ends of the pedicle.

Figure A.2: *The pedicle model. a) The two polylines that describe the 2D shape of the pedicle. b) The 3D model of the pedicle including cross sections at the isthmus and both ends of the pedicle.*

Appendix B: Concept Prototype Experiments

B.1. Experiment Goal

The aim of this experiment is to be able to quantitatively compare the resistance to toggling of the different concept prototypes. Similar papers use cyclic loads to simulate the forces that occur when the anchor is placed in the vertebra [32, 22]. This requires a complex setup with an actuator applying these cyclical loads. This experiment, however, should be as simple as possible in this stage of the research while still getting a quantitative comparison of the different prototypes. Therefore, the choice was made to reduce the experimental load to one linear increasing caudal or cephalad load. From this load and the resulting displacement the resistance torque of the different concept prototypes can be determined. At the same time, this experiment is a proof-of-concept experiment and can show where the flaws are in the different design concepts.

The goal of the experiments is therefore: (1) Evaluate the performance of the three different concepts in terms of rotational resistance torque [Nm]. (2) determine whether the different working principles are feasible and what issues might occur during further development of these concepts.

B.2. Experiment Variables

B.2.1. Independent Variables

Prototypes

For this experiment the three different concept prototypes explained in Section 3.3 are used (Figure B.2. The three different prototypes were 3D printed out of Tough 1500 resin using a Formlabs Form 3. This resin was chosen for its resilient material behavior and cured for half of the recommended time (30 min.) to maintain some flexibility in the material.

B.2.2. Dependent Variables

Resistance Force

The resistance force of the prototype to rotation is equal to the measured input force. This force is a suitable variable to compare the resistance against toggling for all prototypes, because the arm of all test pieces is equally long. Since the goal is to reduce the movement of the in-pedicle anchor the maximum force should be known when the concept prototypes starts to toggle. For this a threshold of 0.5 degrees is chosen.

B.3. Experimental Facility

The experimental facility consists of the 3D-printed pedicle model clamped to a stable surface with the anterior hole directed upwards. The different prototypes were inserted in this pedicle and expanded to simulate the expansion in the pedicle.

Test pieces

The different prototypes have different lengths. To be able to compare the prototypes fairly, the prototypes are prepared in the same way. This means that the centers of the different prototypes and the attachment points for the different sensor were kept the same (Figure B.1c). The arm of the applied force is in all three test pieces 5cm.

Pedicle model

The prototypes are inserted and expanded in the simplified pedicle model that is described in Appendix A. This model was 3D-printed on a Creality Ender 3 Pro out of generic PLA. Only the pedicle cortex was printed and no cancellous bone was used for this first experiment.

Sensors

The displacement angle was measured using a Seika NG4i Inclinometer and the applied input force was measured with a Futek 45N mini loadcell. A measurement amplifier (Scaime CPJ Rail) and DAQ device (NI USB-6008) were used to connect the sensors to a laptop running NI Labview 2018. How the sensors are connected can be seen in Figure B.1a and b.

B.4. Experiment Protocol

After the experimental facility was prepared the different concept prototypes where one by one inserted into the pedicle model and tested. The test piece was inserted into the pedicle, the middle line of the test piece and the pedicle were aligned and the prototype was expanded by tightening the nuts on both sides of the test piece. To make sure that the leverage arm to the center of the test piece was consistent for all three prototypes the nuts on both sides were tightened one turn alternately.

The tightening was stopped when then prototypes were visually expanded fully. Because the prototype had the tendency to slide in the pedicle model and adapt their position and shape to the surrounding pedicle the position and length of the prototype were measured after the expansion to be able to accurately replicate the experiment. Together with these measurements the force and angle offsets of the sensors were noted for each prototype.

First on each prototype the load cell was aligned for a pulling force in the cranial direction. The force was applied by pulling on a string attached to the load cell. This force was as consistently as possible increased to a maximum of around 25N. After this the string was slowly released. Next the force sensor was rotated 180 degrees to allow the application of a pulling force in the caudal direction on the same prototype. Again the

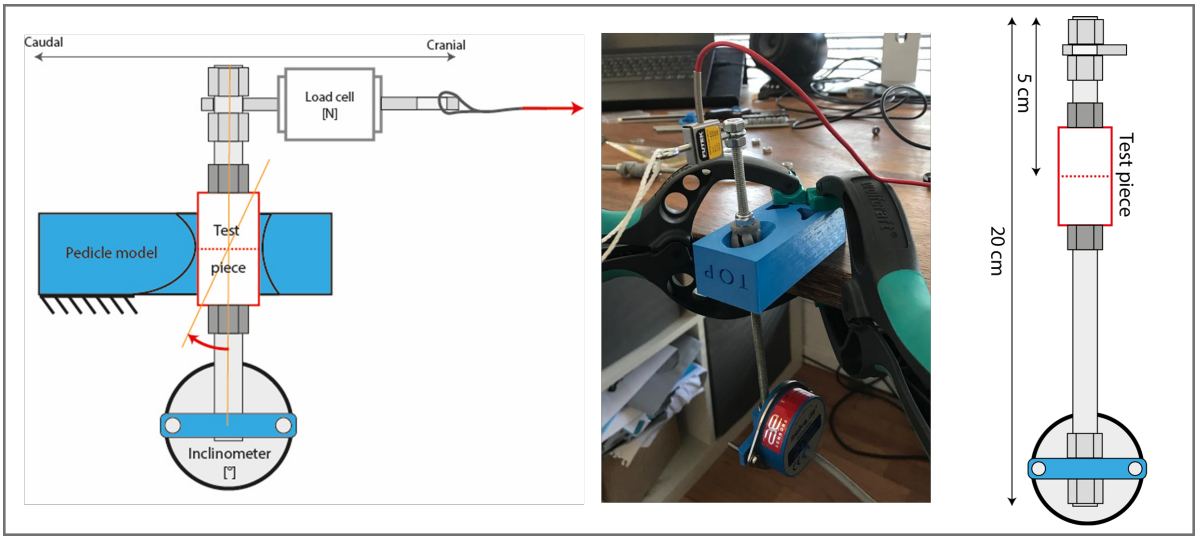

Figure B.1: *The experimental facility of the concept prototype lateral loading experiment. a) Sketch of the test setup including the sensors. b) Photograph of the setup. c) Sketch and dimensions of the test pieces*

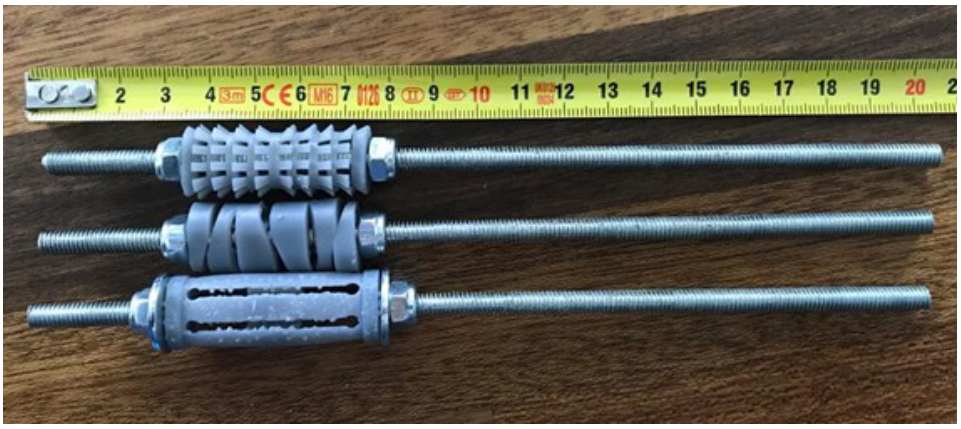

Figure B.2: *The three different prototype test pieces*

force and angle offsets were noted. The same force buildup was used as well.

B.5. Data Analysis

The data out of NI Labview was converted to a Matlab input. The input force and output displacement were plotted and the input torque at the threshold angle of 0.5° was determined. All data analysis was performed with MATLAB R2021b.

B.6. Results

B.6.1. Quantitative results

The raw displacement and force data from the experiments for both caudal and cranial forces are plotted in Figure B.4 including the 0.5 degree threshold line. The determined threshold forces are summarized in Table B.1.

B.6.2. Qualitative results

The state of the concept prototypes after the experiment can be seen as qualitative results. The deformations or lack thereof can show whether the prototypes were able to withstand the lateral forces and input torque of the nut. Therefore, the images of the prototypes are included in Figure B.4.

B.7. Discussion

B.7.1. Main Findings

The data from this concept prototype experiment shows that the plug concept prototype is the least stiff system of the three. This can be explained by the long flexible parts. These results were confirmed by inspecting the prototype after the experiment (see Figure B.3c). The prototype was completely deformed due to the lateral loads. Moreover the concept was heavily twisted due to the rotation friction induced by the nut, even when a washer was used.

(a) *Star concept Prototype after the experiment*

(b) *Wedge concept Prototype after the experiment*

(c) *Plug Prototype after the experiment*

Figure B.3: *Photos of concept prototypes after the lateral loading experiment*

The star concept prototype shows that many flexible parts that are compressed can result in a relatively rigid system. It almost matches the results of the wedge concept in the caudal direction and is more stiff in the cranial direction. The photos of the star concept prototype in Figure B.3a show that the small protrusions require great deformations to fixate in the model. However, the great stresses that would occur in a metal variant combined with these small protrusions may result in small parts becoming detached. This can lead to dangerous situations when implanted in the body and thereby violates the set requirements.

Although all three prototypes can be improved a lot, the wedge concept prototype seems the most promising for further development. Possible improvements for the wedges prototype lays in achieving a controlled expansion. The expansion of the wedge concept prototype was unpredictable and messy, but still resulted in a rather stiff fixation. This was caused by the ability of each wedge to move in the vertical and horizontal directions at the same time. In addition, the expansion parts can rotate around the round central screw, which makes this effect even worse. This phenomenon is clearly visible in the photo made after the experiment in Figure B.3b.

It is also striking that this prototype works much better in the caudal direction than the cranial direction. This could be caused by the chaotic unfolding, but this difference is most probably caused by the asymmetrical shape of the internal pedicle. This may not be a problem, because the greatest forces in the back are in the caudal direction [27], but sufficient support also should be provided in the cranial direction.

B.7.2. Limitations

The small sample size makes that no statistical analysis can be used on the data. This means that no statistically relevant conclusion can be drawn but the experiment gives an indication of the functioning of the different prototypes to support the argumentation for choosing one of the prototypes. There is no experimental data from papers that can be compared to the outcomes of this experiment, but this was not the goal either. The data of the three prototype can be compared.

The different prototypes had the tendency to slide inside the pedicle model during the expansion, this makes the measurements hard to replicate. During the experiment the input force was applied with a string directly by hand. As a results, the input force graph was not a fluent line, but the force had some fluctuations around the linear increment. A more consistent force input would result in a more consistent output angle, which would make the determination of the force at the angle threshold more accurate.

B.8. Conclusion

During this concept prototype experiment three concepts were compared based on their resistance to lateral forces (caudal and cranial). The experiment using a setup consisting of a pedicle model, the concept prototypes, an inclinometer and a load cell showed that the star concept prototype is the most consistent in both directions, but needs high displacements of the small protrusion to fixate in the pedicle. The wedge prototype is the most resistant to caudal forces and therefore a promising concept. However, the chaotic expansion of this concept and the worse performance against cranial forces will have to be investigated more.

	Prototype 1: Star		Prototype 2: Wedges		Prototype 3: Plug	
	Cranial	Caudal	Cranial	Caudal	Cranial	Caudal
Force [N]	7.305	9.992	3.894	11.022	3.862	4.167

Table B.1: *Cranial and Caudal forces for the three different concept prototype at a 0.5 degree displacement*

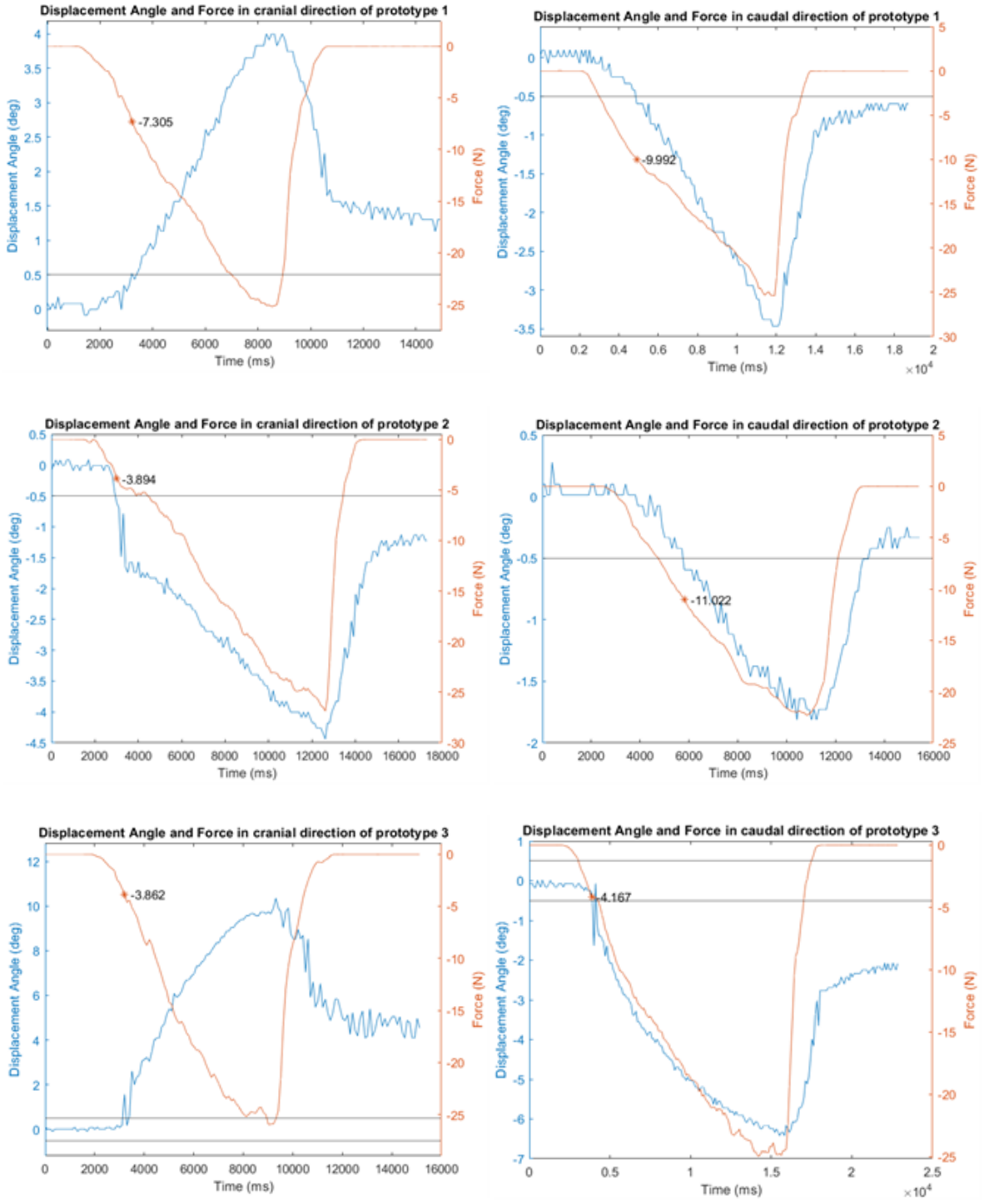

Figure B.4: *Resulting force displacement graphs of the concept prototype lateral loading experiment.*

Appendix C: Friction Calculations

C.1. Self-Locking calculation

To see if a potential prototype is able to expand, the bone resistance force can be omitted. In this way, we can determine what the relation is between the inclination angle of the wedge and the maximum coefficient of friction the used material can have. By looking at the free body diagram displayed in Figure C.1 we get the equations C.1, C.2 and C.3 that combined lead to equation C.4.

$$W = F_{in} * sin(\alpha) \tag{C.1}$$

$$N = F_{in} * cos(\alpha) \tag{C.2}$$

$$W = N * \mu \tag{C.3}$$

$$\mu = \frac{F_{in} * sin(\alpha)}{F_{in} * cos(\alpha)} = tan(\alpha) \tag{C.4}$$

This final equation C.4 gives the maximum coefficient of friction for a certain inclination angle of the wedge before self-locking occurs. Self-locking occurs when two wedges won't move with respect to each other independent of the input force due to a friction force that is too large. If we take the inclination angle of our prototype, which is α=7.5°, the resulting maximum Coefficient of Friction (CoF) is μ = 0.13.

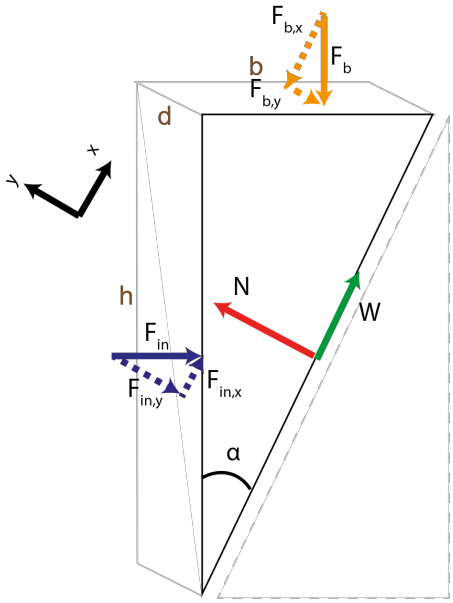

Figure C.1: *Free Body Diagram of prototype wedge including normal force (N), friction force (W), input force (F_{in}) and bone resistance force (F_{bone})*

C.2. Calculation of input forces due to friction

Although self-locking is an important aspect to consider in this design it is not sure that the prototype will function when there is no self-locking. Even when the inclination angle is higher than the minium angle, high input forces may still be required due to friction. To show whether this is the case the force on a wedge are modelled, this time including the bone resistance force.

By including this force a relation between the input force and the force needed to compress the bone can be determined. By determing the force equilibrium in the x-direction (Equation C.5) and y-direction (Equation C.6) and combining this with the general relation between the normal and friction force (Equation C.7) we can calculate this input force. This results in Equation C.8.

$$W = F_{in} * \sin(\alpha) - F_b * \cos(\alpha) \tag{C.5}$$

$$N = F_{in} * \cos(\alpha) + F_b * \sin(\alpha) \tag{C.6}$$

$$W = N * \mu \tag{C.7}$$

$$F_{in} = F_b * \frac{\mu * \sin(\alpha) + \cos(\alpha)}{-\mu * \cos(\alpha) + \sin(\alpha)} \tag{C.8}$$

The force needed to compress the bone (F_b) can be easily calculated by multiplying the top area of the wedge with the compression strength ($f_{compress}$). Both the equations were combined to get the final equation that couples the required input force to the inclination angle for a certain set CoF. This resulting equation is visualized in Figure C.2 for multiple values of the CoF. In this graph the asymptotes for each CoF show the effect of self-locking that is described on the previous page. The asymptotes represent the minimum angle before self-locking occurs. The graph shows that an inclination angle that is too close to the minimum angle can lead to high required input forces.

$$F_{in} = f_{compress} * A_{top} * \frac{\mu * \sin(\alpha) + \cos(\alpha)}{-\mu * \cos(\alpha) + \sin(\alpha)} \tag{C.9}$$

C.3. Calculation of Sliding surface pressures

To verify whether the the surface pressure on the wedge sliding surface is lower than friction surfaces in other applications we need to calculate this value. This can be done by using Equations C.10 and C.11.

$$N = F_b/(\sin(\alpha) - \mu * \cos(\alpha)); \tag{C.10}$$

$$P = N/A \tag{C.11}$$

The surface pressure that occurs is influenced by the inclination angle, CoF of the prototype material and by

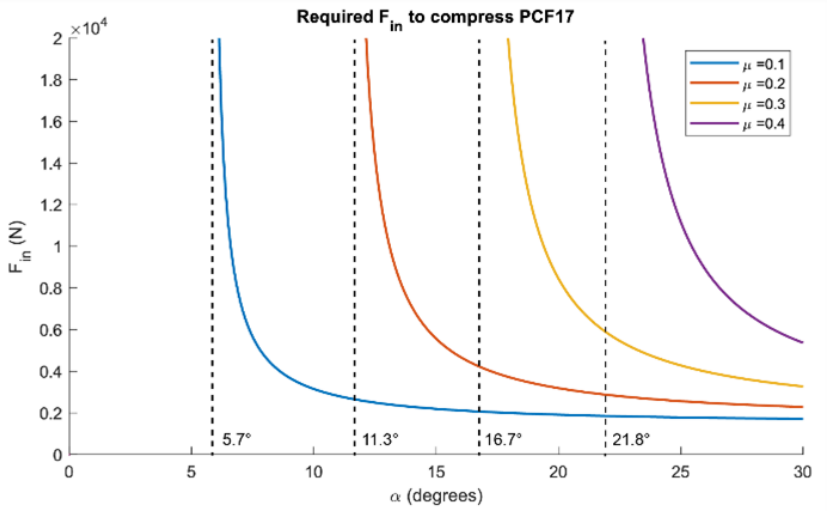

Figure C.2: *Graph of the required input force to compress 17pcf Sawbones bone foam including the friction asymptotes*

the compression strength of the used solid bone foam. To get a ball-park estimate of the occuring surface pressures we assumed an inclination angle α of 7,5°, a CoF (μ) of 0.1. The surface pressures were calculated for all available bone densities from 5 to 17 PCF solid foam. The resulting pressures are noted in Table C.1.

C.4. Calculation of Bolt Nut surface pressures

We assume a M6 bolt that has a lead length (L) of 1mm, a CoF μ of 0.1, a major (d_{maj}), minor (d_{min}) and thread diameter (d_m) of respectively 5, 6 and 5.35mm that engages with five windings (N) of a M6 nut. The total torque T_t that is applied is 10 Nm. Figure C.3 shows a single thread winding and the forces that apply on this part when a force opposes the movement direction [39].

$$\alpha = arctan(L/(\mu * d_m)) \quad \text{(C.12)}$$

$$T_t = W * r_m * \tan(\alpha + atan(\mu)) \quad \text{(C.13)}$$

From Equation C.12 we can determine that the lead angle α is 3.4°. Inputting this with the other inputs in Equation C.12 leads to a total clamping force W of 11670 N.

$$A = N * (\pi * ((d_{maj}/2)^2 - (d_{min}/2)^2)) \quad \text{(C.14)}$$

The total pressure surface is based of five windings and can be calculated by using Equation C.14. This leads to a total pressure surface of 43.2mm^2. The total contact pressure is therefore:

$$P = W/A = 11670N/43.2mm^2 = 270MPa \quad \text{(C.15)}$$

This makes the surface pressures on the wedges in 5 PCF bone foam around 100 times smaller than the surface pressure in our example M6 bolt-nut connection. For 10 PCF bone foam is this around 30 times smaller.

Table C.1: *Calculated surface pressures of wedges.*

	Surface Pressure (MPa)
5 PCF	2.5
10 PCF	9.2
15 PCF	20.6
17 PCF	26.0

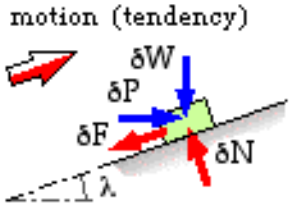

Figure C.3: *Free Body Diagram of single thread unit including forces [39].*

Appendix D: Raw Data Validation Experiments

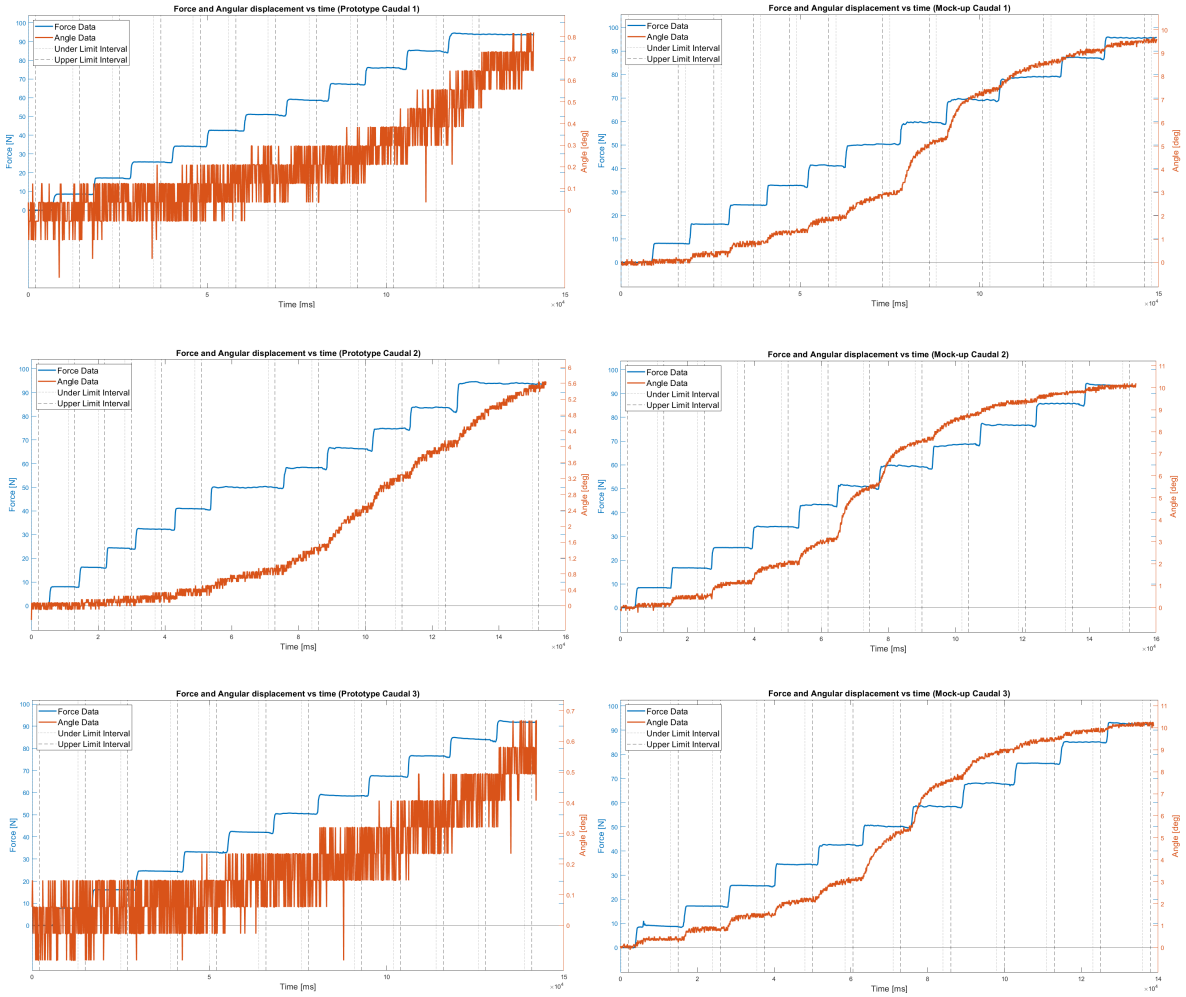

Figure D.1: *Caudal Raw data from Experiment 2: In-pedicle expansion and loading experiment.*

Table D.1: *Angular displacement at maximum load for caudal force*

	Test 1	Test 2	Test 3	AVG	STD
Prototype	0.6	5.5	0.6	2.2	2.3
Mockup	9.5	10.1	10.2	9.9	0.3

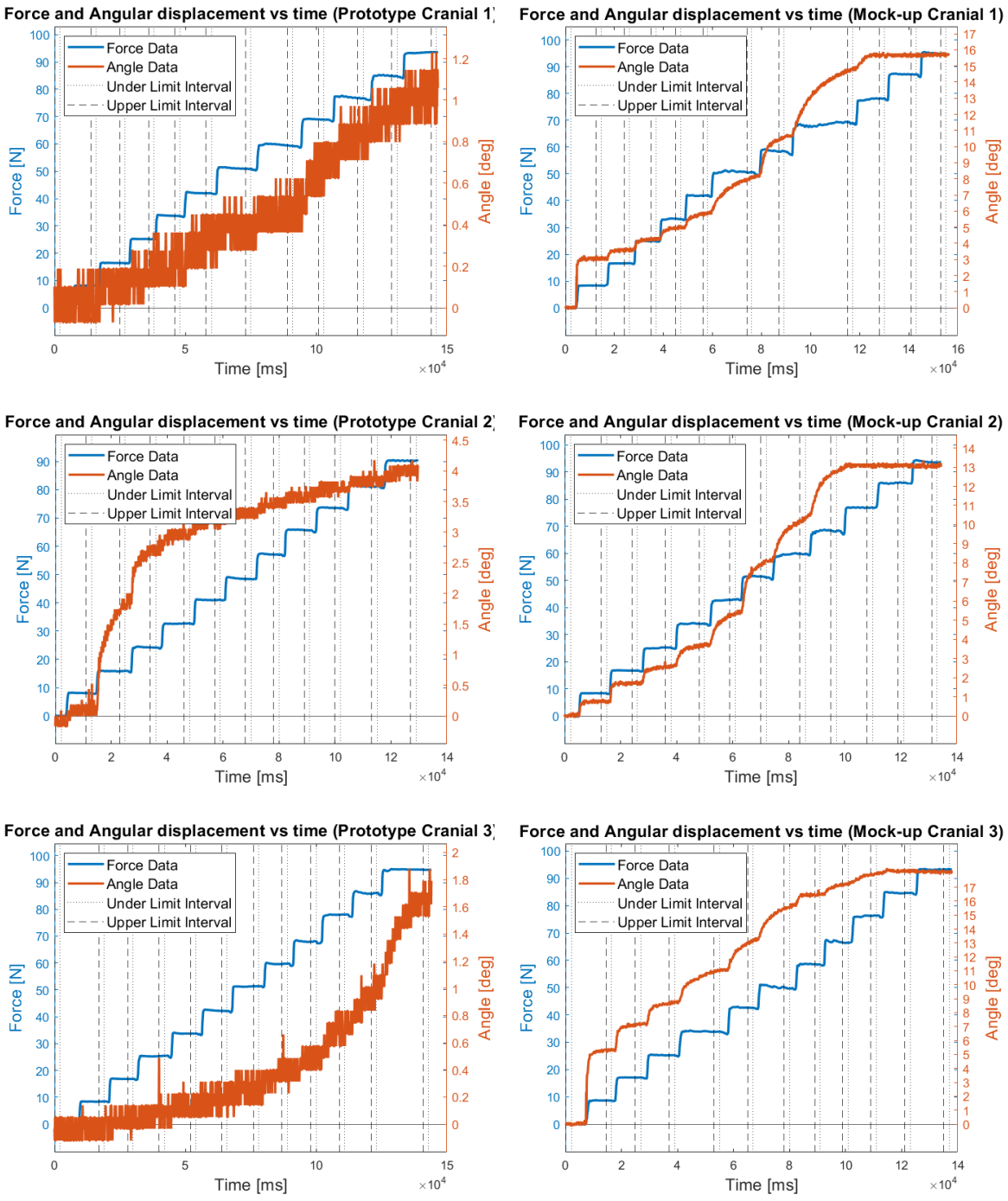

Figure D.2: *Cranial Raw data from Experiment 2: In-pedicle expansion and loading experiment.*

Table D.2: *Angular displacement at maximum load for cranial force*

	Test 1	Test 2	Test 3	AVG	STD
Prototype	1.0	4.0	1.6	2.2	1.3
Mockup	15.7	13.0	18.1	15.6	2.1

Appendix E: Technical Drawings Final Prototype

E.1. Overview

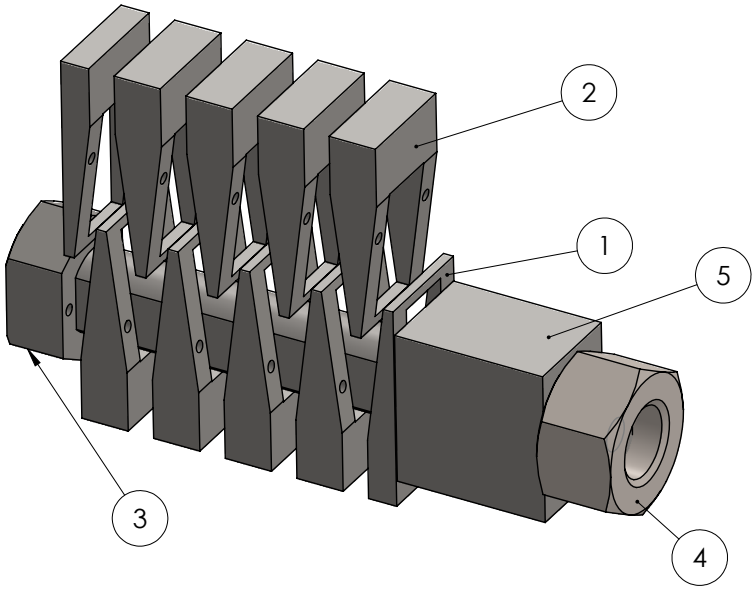

ITEM NO.	PART NUMBER	QTY.
1	End Wedge	2
2	Middle Wedge	8
3	Modified Hex bolt M8 x 1.25 x 40	1
4	Hex nut, Style 2, M8 x 1.25 --D-N	1
5	Extension Tube	1

MATERIAL: Stainless Steel (316L)	In-Pedicle Anchor	A4
WEIGHT:	SCALE:2:1	SHEET 1 OF 2

E.2. End Wedge

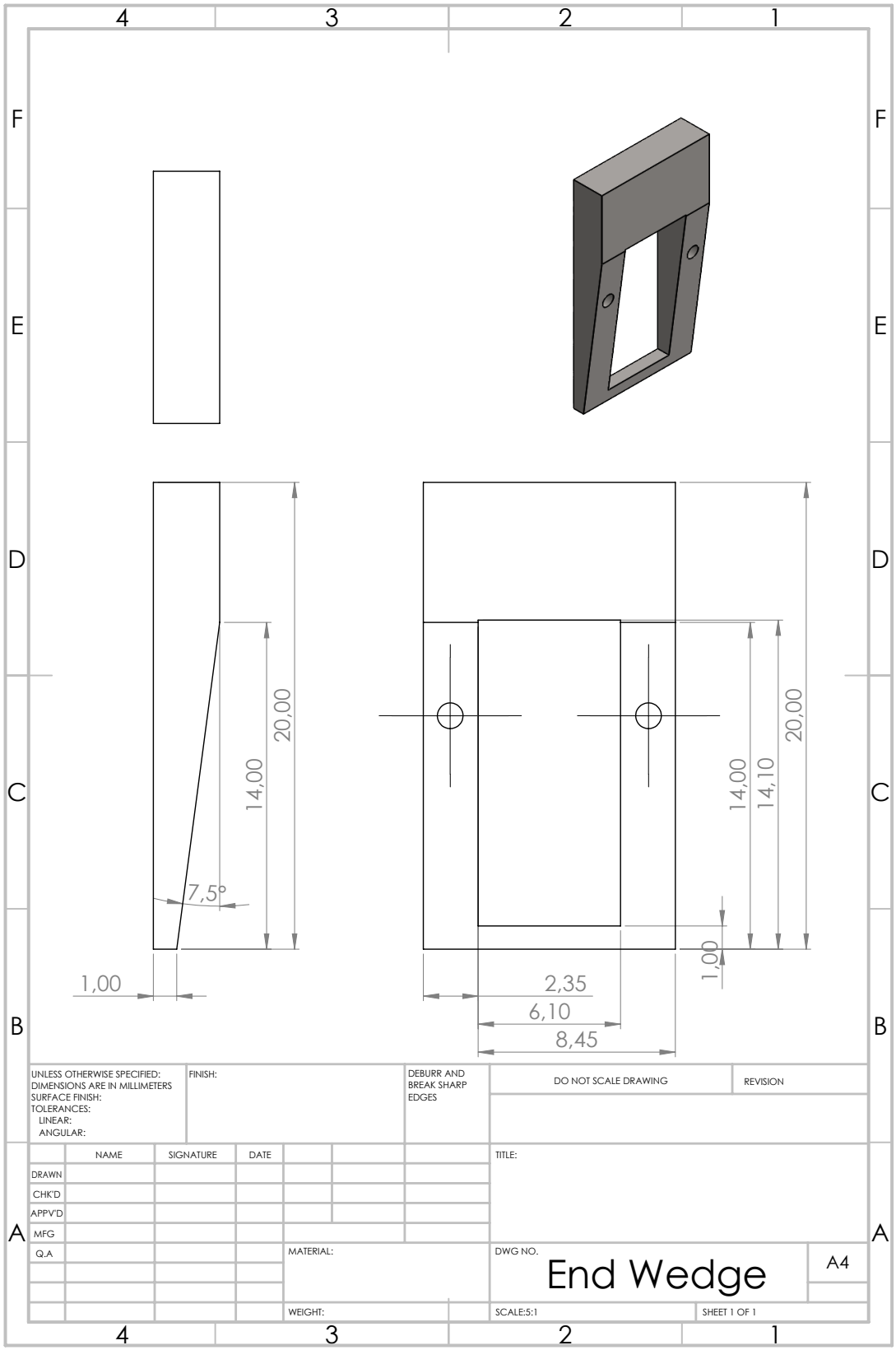
4
3
2
1
F
E
D
C
B
A
20,00
14,00
7,5°
1,00
14,00
14,10
20,00
1,00
2,35
6,10
8,45
UNLESS OTHERWISE SPECIFIED:
DIMENSIONS ARE IN MILLIMETERS
SURFACE FINISH:
TOLERANCES:
LINEAR:
ANGULAR:
FINISH:
DEBURR AND BREAK SHARP EDGES
DO NOT SCALE DRAWING
REVISION
NAME
SIGNATURE
DATE
DRAWN
CHK'D
APPV'D
MFG
Q.A
TITLE:
MATERIAL:
DWG NO.
End Wedge
A4
WEIGHT:
SCALE:5:1
SHEET 1 OF 1

E.3. End Wedge

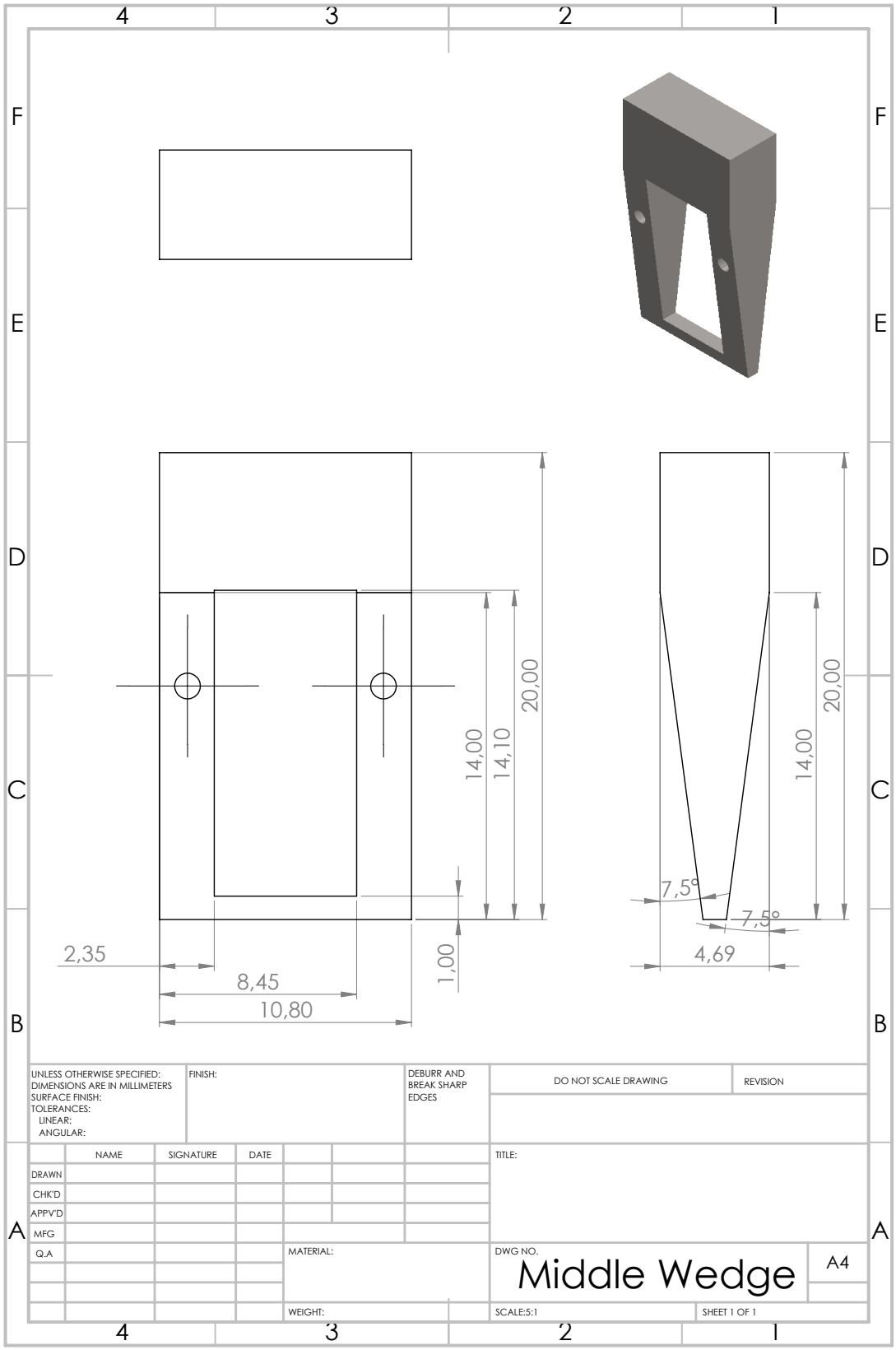
20,00
14,00
14,10
2,35
8,45
10,80
1,00
7,5°
7,5°
4,69
UNLESS OTHERWISE SPECIFIED:
DIMENSIONS ARE IN MILLIMETERS
SURFACE FINISH:
TOLERANCES:
LINEAR:
ANGULAR:
FINISH:
DEBURR AND BREAK SHARP EDGES
DO NOT SCALE DRAWING
REVISION
NAME
SIGNATURE
DATE
DRAWN
CHK'D
APPV'D
MFG
Q.A
TITLE:
MATERIAL:
DWG NO.
Middle Wedge
A4
WEIGHT:
SCALE:5:1
SHEET 1 OF 1

E.4. Central Bolt

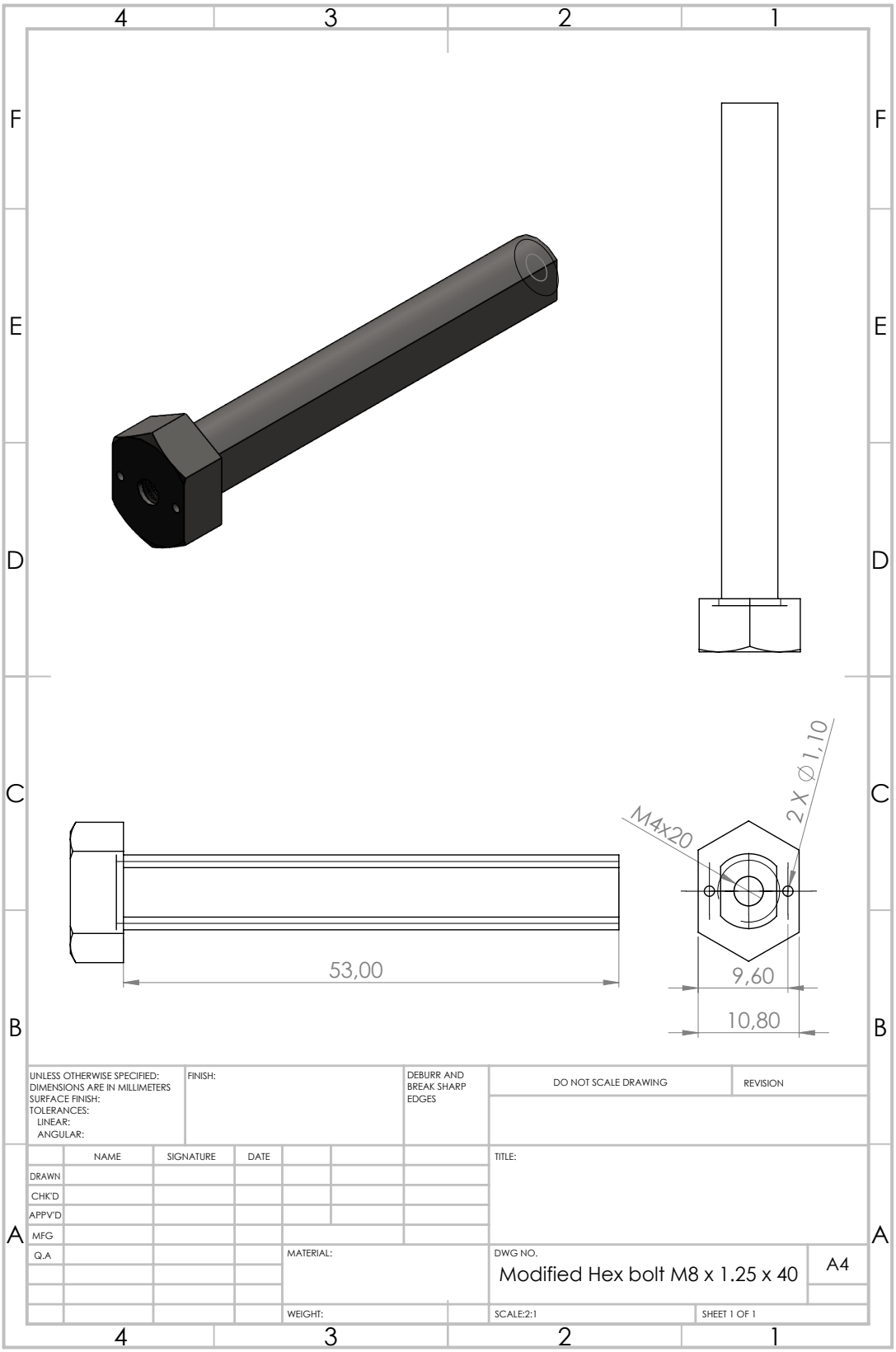

E.5. Extension Tube